

Classification and Comparison of Massive MIMO Propagation Channel Models

Rui Feng^{1b}, *Member, IEEE*, Cheng-Xiang Wang^{1b}, *Fellow, IEEE*, Jie Huang^{1b}, *Member, IEEE*, Xiqi Gao^{1b}, *Fellow, IEEE*, Sana Salous^{2b}, *Senior Member, IEEE*, and Harald Haas^{3b}, *Fellow, IEEE*

Abstract—Considering great benefits brought by massive multiple-input–multiple-output (MIMO) technologies in the Internet of Things (IoT), it is of vital importance to analyze new massive MIMO channel characteristics and develop corresponding channel models. In the literature, various massive MIMO channel models have been proposed and classified with different but confusing methods, i.e., physical versus analytical method and deterministic versus stochastic method. To have a better understanding and usage of massive MIMO channel models, this work summarizes different classification methods and presents an up-to-date unified classification framework, i.e., artificial intelligence (AI)-based predictive channel models and classical nonpredictive channel models, which further clarify and combine the deterministic versus stochastic and physical versus analytical methods. Furthermore, massive MIMO channel measurement campaigns are reviewed to summarize new massive MIMO channel characteristics. Recent advances in massive MIMO channel modeling are surveyed. In addition, typical nonpredictive massive MIMO channel models are elaborated and compared, i.e., deterministic models and stochastic models,

which include the correlation-based stochastic model (CBSM), geometry-based stochastic model (GBSM), and beam-domain channel model (BDCM). Finally, future challenges in massive MIMO channel modeling are given.

Index Terms—Artificial intelligence (AI)/machine learning (ML)-based predictive channel models, beam-domain channel model (BDCM), correlation-based stochastic model (CBSM), geometry-based stochastic model (GBSM), massive multiple-input–multiple-output (MIMO) channel models.

I. INTRODUCTION

FUTURE sixth-generation (6G) system aims to fulfill highly demanded wireless communication requirements and visions [1], [2]. It will be an intelligent network that links humans, robots, smart cars, medical devices, industry equipments, etc., together to accomplish ultra reliable low-latency Internet of Things (IoT) paradigm shift. However, the massive access and low-cost real-time interactions of sensors/systems pose huge challenges to 6G intelligent IoT. Massive multiple-input–multiple-output (MIMO) [3], which equips tens, hundreds, or even thousands of individual antennas at the base station (BS) to serve tens of user equipment (UE) simultaneously, can significantly improve energy efficiency (EE), spectrum efficiency (SE), and system capacity of IoT. In view of the great benefits brought by massive MIMO, it can be used at sub-6 GHz, millimeter wave (mmWave), terahertz (THz), and optical wireless frequency bands, and can be incorporated in different IoT communication scenarios to provide reliable communications [4], [5], [6], [7], [8], [9], [10].

To design and evaluate performance of wireless communication system, channel modeling has always played a pivotal role, as illustrated in Fig. 1. Great efforts have been done in channel modeling to pursue more accurate description of wireless channels, especially to follow the drastic development of wireless communication technologies. In IoT scenarios, the channel shows varied path loss, random fluctuations, nonline-of-sight (NLoS) propagation, large amounts of scatterers, and multimobility. Inevitably, along with the dramatic increase of antenna array size, new propagation channel characteristics appear in massive MIMO channels. In order to choose suitable channel model and provide accurate description of new massive MIMO channel characteristics, further considering the convenience for channel estimation, system performance analysis, etc., it is of great value to clarify different channel modeling methodologies as well as their pros and cons. There are many channel models proposed abiding by different

Manuscript received 25 December 2021; revised 21 May 2022; accepted 26 July 2022. Date of publication 16 August 2022; date of current version 21 November 2022. This work was supported in part by the National Key Research and Development Program of China under Grant 2020YFB1804901; in part by the National Natural Science Foundation of China (NSFC) under Grant 6196206006 and Grant 61901109; in part by the Key Technologies Research and Development Program of Jiangsu (Prospective and Key Technologies for Industry) under Grant BE2022067 and Grant BE2022067-1; in part by the Frontiers Science Center for Mobile Information Communication and Security; in part by the Research Fund of National Mobile Communications Research Laboratory, Southeast University under Grant 2021B02; in part by the EU H2020 RISE TESTBED2 Project under Grant 872172; in part by the Jiangsu Province Basic Research Project under Grant BK20192002; in part by the Fellowship of China Postdoctoral Science Foundation under Grant 2021M690628; in part by the Natural Science Foundation of Shandong Province under Grant ZR2019PF010; in part by the High Level Innovation and Entrepreneurial Doctor Introduction Program in Jiangsu under Grant JSSCBS20210082; in part by the Fundamental Research Funds for the Central Universities under Grant 2242022R10067; and in part by the EPSRC Established Career Fellowship Prof. Haas under Grant EP/R007101/1. (*Corresponding author: Cheng-Xiang Wang.*)

Rui Feng is with the Pervasive Communication Research Center, Purple Mountain Laboratories, Nanjing 211111, China, and also with the School of Information Science and Engineering, Southeast University, Nanjing 210096, China (e-mail: fengxiurui604@163.com).

Cheng-Xiang Wang, Jie Huang, and Xiqi Gao are with the National Mobile Communications Research Laboratory, School of Information Science and Engineering, Southeast University, Nanjing 210096, China, and also with the Pervasive Communication Research Center, Purple Mountain Laboratories, Nanjing 211111, China (e-mail: chxwang@seu.edu.cn; j_huang@seu.edu.cn; xqgao@seu.edu.cn).

Sana Salous is with the School of Engineering and Computing Sciences, Durham University, Durham DH1 3LE, U.K. (e-mail: sana.salous@durham.ac.uk).

Harald Haas is with the LiFi Research and Development Center, University of Strathclyde, Glasgow G1 1XQ, U.K. (e-mail: harald.haas@strath.ac.uk).

Digital Object Identifier 10.1109/JIOT.2022.3198690

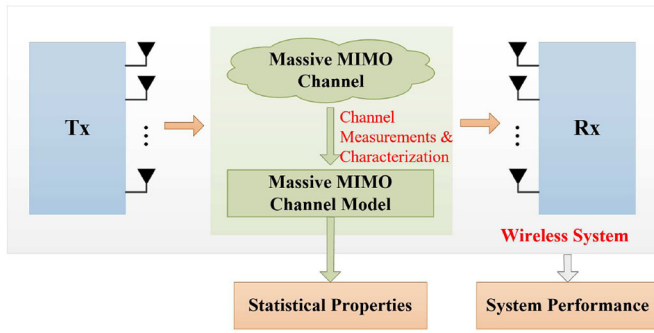


Fig. 1. Importance of massive MIMO channel modeling.

methodologies. This survey contributes to clarify the methodologies and specialties of different channel models, especially to unravel their potentials in the face of new massive MIMO channel characteristics. This will be accomplished in two steps: 1) classification and 2) comparison.

As the most intuitive way to understand wireless channels, channel measurements are often carried out in the time or frequency domain to acquire measurement data for certain communication scenarios [11]. The channel impulse response (CIR) or channel transfer function (CTF) can then be obtained based on multipath component (MPC) parameters extracted by using data postprocessing algorithms, such as multiple signal classification (MUSIC) [12] and space-alternating generalized expectation-maximization (SAGE) [13], [14], [15] algorithms. To reduce costs of channel measurements, ray-tracing (RT) can be used to simulate the electromagnetic wave propagation [16]. Besides channel measurements and RT, there are also correlation-based stochastic models (CBSMs), geometry-based stochastic models (GBSMs), artificial intelligence (AI)/machine learning (ML)-based channel models, etc. GBSMs need to carefully design the CIR with parameters calculated according to geometrical relationships among the transmitter (Tx), receiver (Rx), and scatterers. CBSMs are derived from temporal and spatial correlation matrices. AI/ML-based channel models are trained with extensive measurement or simulation data samples to predict channel statistics for unknown channels. Some channel models are standardized by international organizations for practical applications, such as the European cooperation in the field of scientific and technical research (COST) 2100 [17], 3rd generation partnership project (3GPP) spatial channel model (SCM) [18], wireless world initiative for new radio (WINNER) II/+ [19], [20], millimeter-wave evolution for backhaul and access (MiWEBA) [21], quasideterministic radio channel generator (QuaDRiGa) [22], etc. However, it will be shown in this article that most existing channel models fail to consider complete new characteristics of massive MIMO channels.

In the literature, different methods have been proposed to classify channel models. For instance, there are narrowband versus wideband channel models, stationary versus nonstationary channel models, and channel models based on different communication scenarios such as vehicle-to-vehicle (V2V), high speed train (HST), unmanned aerial vehicle (UAV), satellite, and maritime channel models [23]. The aforementioned classification methods are simple and not sufficient to give

an utmost separation of various channel models. Another two popular classification methods are physical versus analytical [24], [25] and deterministic versus stochastic [23] ones. The former method is categorized by model parameters either physically based or mathematically/analytically based, while the latter method is classified by model parameters containing either only fixed values or random variables. However, it will be shown in this article that the above two methods fail to include the latest channel models such as AI/ML-based channel models. Also, the physical versus analytical method is unable to provide exclusive classifications of channel models. Furthermore, channel models with essentially the same methodology but different names should be unified. For example, the newly proposed beam-domain channel models (BDCMs) are constructed by transforming traditional channel models from the array domain to beam domain [26], [27], [28]. It follows the same methodology as the virtual channel representation (VCR) [29].

In terms of comparison, the performance of channel models can be measured by three key performance indicators (KPIs), i.e., accuracy, complexity, and pervasiveness/universality [1]. Accuracy is an important indicator to measure to what extent the real channel is reproduced by a channel model. This includes the comparison between the real channel and a channel model regarding new channel characteristics. Complexity is to measure the operations used for channel model generation and affected by many factors, such as parameter computation methods, numbers of parameters and CIR samples, etc. Pervasiveness/universality means that the proposed channel models should be adaptive to various frequency bands and various communication scenarios by adjusting channel model parameters. It is important to mention that the aim of designing channel models is to get the optimum tradeoff among these three KPIs. There are only few papers regarding the comparison of various channel models in terms of the above KPIs [30], [31], [32], [33], [34], [35], [36], [37], [38], [39]. Previous comparisons mainly focused on two kinds of traditional MIMO channel models, i.e., Kronecker-based stochastic models (KBSMs) and GBSMs, in terms of their accuracy and complexity [40]. To the best of our knowledge, a thorough comparison of massive MIMO channel models considering all the three KPIs is still missing in the literature.

A. Existing Surveys and Tutorials

In the literature, there are some survey papers that emphasize on different aspects of wireless channel models. We summarize related survey papers in Table I. In [25], [41], and [42], physical, analytical, and standardized MIMO channel models were briefly reviewed. The benefits and limitations of MIMO channel models were given in [42]. In [1] and [43], available small-scale channel models, divided into deterministic and stochastic models, were summarized for different 6G frequency bands and scenarios. In [44], RT, map-based, point cloud, quasideterministic, Saleh-Valenzuela (SV), propagation graph, and GBSM were classified into deterministic, semideterministic, and stochastic channel models. In [45], mmWave channel propagation challenges were introduced,

TABLE I
RELATED SURVEYS ON WIRELESS CHANNEL MODELS

Ref.	Brief summary
[25], [41], [42]	A survey of physical, analytical, and standardized MIMO channel models
[1], [43]	A survey of 6G oriented wireless communication channel models
[44]	Investigation of deterministic, semi-deterministic, and stochastic mmWave channel models
[45]	Review of standardized mmWave channel models
[46]	Review of deterministic, statistical, hybrid THz channel models in single-antenna and ultra-massive MIMO systems
[47], [48]	An overview of HST channel measurements and models
[49]	Review of deterministic and statistical massive MIMO channel models, RT and GBSM mainly
[3], [50], [51]	Review of GBSMs and CBSMs in massive MIMO communication systems

standard channel models including the Line-of-Sight (LoS) model, large-scale path loss models, outdoor-to-indoor penetration loss, and spatial consistency were summarized. In [46], deterministic, statistical, hybrid THz channel models in single-antenna and ultramassive MIMO systems were reviewed. There are also survey papers about recent developments of HST channel models [47], [48]. In terms of massive MIMO channel models, recent advances of deterministic channel models, including RT and map based, as well as stochastic channel models, including GBSM, were discussed in [49]. In [3], CBSMs including independent and identically distributed (i.i.d.) Rayleigh, correlation, and mutual coupling channel models, and GBSMs including two-dimensional (2-D) and three-dimensional (3-D) channel models were introduced. It can be seen from the above mentioned surveys that a unified classification framework considering the latest massive MIMO channel models is absent. Also, there lacks a comprehensive comparison of various massive MIMO channel models.

B. Main Contributions and Organization

To fill the above gaps, this article elaborates on the classification and comparison of different massive MIMO channel models. The main contributions of this work are summarized as follows.

- 1) Two massive MIMO channel model classification methods, i.e., physical versus analytical and deterministic versus stochastic methods, are introduced and compared. Then, a unified predictive versus nonpredictive channel model classification framework is proposed aiming for a more coherent, completer, and exclusive classification methodology.
- 2) Massive MIMO channel characteristics analyzed based on channel measurement campaigns are summarized. Fundamentals and recent advances of massive MIMO channel models considering new characteristics are detailed reviewed comprehensively.
- 3) Comparisons of different massive MIMO channel models are given in terms of three KPIs, i.e., accuracy, complexity, and pervasiveness/universality.
- 4) Future challenges of massive MIMO channel modeling are pointed out.

The remainder of this article is organized as follows. In Section II, the wireless channel model classification methods are introduced and a unified classification framework is

proposed. In Section III, massive MIMO channel characteristics are surveyed and fundamentals of several channel models are introduced. In Section IV, comparisons of classical massive MIMO channel models are presented. Future challenges are summarized in Section V. Finally, conclusions are drawn in Section VI.

II. WIRELESS CHANNEL MODEL CLASSIFICATIONS

A. Physical Versus Analytical Channel Model Classification

The classification of physical and analytical channel models depicted in Fig. 2 can be referred to [25]. They are classified by model parameters either physically propagation based or mathematically/analytically based.

In wireless channels, caused by reflection, scattering, and diffraction mechanisms, signals transmitted from Tx and impinged at Rx may experience multipath propagation. MPCs should have different parameters including complex amplitude, delay, Azimuth/Elevation Angle of Arrival (AAoA/EAoA), Azimuth/Elevation Angle of Departure (AAoD/EAoD), etc. Channel models characterized based on MPC propagations in array/physical domain are classified as physical model. They aim to reproduce radio propagation without considering the influences of antenna configurations and other system setups. Physical channel models can be further divided into deterministic model, GBSM, and nongeometrical stochastic model (NGSM). If the model is devoted to simulate the actual propagation mechanisms with fixed parameters, it is deterministic. Stored channel measurements and RT can both be used to acquire deterministic channel parameters. GBSM can describe wireless channels based on the basic geometrical relationships among Tx, Rx, and scatterers. Here, NGSM mainly indicates the SV model [52]. In the SV model, it is assumed that MPCs arrive in groups and scatterers can be distinguished as clusters.

Correspondingly, channel models established in a mathematical way are analytical-based. This category of models highly relates to the channel and relies on system setups including bandwidth and antenna array configuration. They are usually used for information theory and signal processing research. Analytical channel models can be subdivided into CBSMs and propagation-motivated model. CBSMs assume the elements of fast fading channel matrix are i.i.d. Gaussian random variables. They are further divided into i.i.d. Rayleigh model, KBSM, and Weichselberger model (WM) based on different simplified spatial full correlation matrices. The i.i.d.

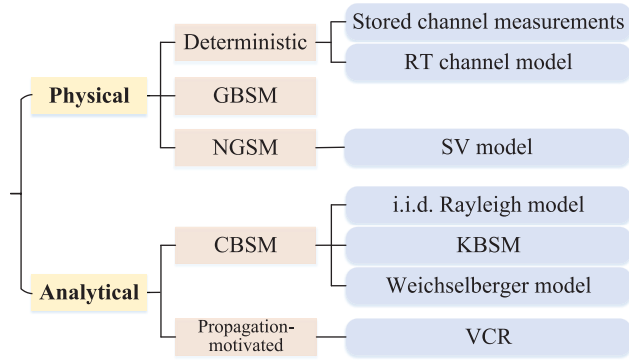


Fig. 2. Physical versus analytical classification methods [25].

Rayleigh model is the simplest one, which assumes that the antenna elements are far located and surrounded by enough scatterers, i.e., no correlation and mutual coupling between Tx and Rx antennas. Then, the elements of full correlation matrix are all equal to one certain value. This model can only be used when MPCs are rich and are distributed uniformly in the spatial domain. The KBSM is formed by separating the Tx and Rx spatial correlation as independent parts. However, [53] showed that it cannot render the MPC structure correctly, thus failed to provide accurate estimation of system capacity. To overcome the drawbacks of KBSM, WM is proposed by considering the mutual coupling between the Tx and Rx spatial correlation property and employing eigenmodes of the Tx and Rx correlation matrices. The WM shows significant modeling accuracy over the KBSM. In Fig. 2, the propagation-motivated model mainly includes VCR. It considers the propagation environment between virtual Tx and Rx directions/beams with the aid of a coupling matrix and discrete Fourier transformation (DFT) matrix. Performance of this model highly relies on the spatial resolution of the antenna array. Note that we unify the naming of VCR as BDCM in the following.

Regarding the clarity of this classification method, it should be mentioned that CBSMs indicate stochastic models without geometrical description. Therefore, CBSMs should also belong to NGSM. In addition, physical models characterize MPC transmission in the array domain, while BDCM characterizes the channel in a virtual beam domain, they are all propagation-motivated models.

B. Deterministic Versus Stochastic Channel Model Classification

The classification of deterministic and stochastic channel models is shown in Fig. 3 [23]. The classification criterion inherent in this method is whether the model parameters are only fixed values or randomly distributed variables.

Deterministic models mean all related parameters are fixed values. Once channel measurements or RT simulations are conducted, MPC parameters and further the CIR/CTF are known for sure. A single realization of a stochastic model, not necessarily ergodic, also belongs to deterministic model. Stochastic models should have at least one parameter that is a random variable. Both GBSMs and NGSMs are classified as stochastic models. They are different in the methodology to

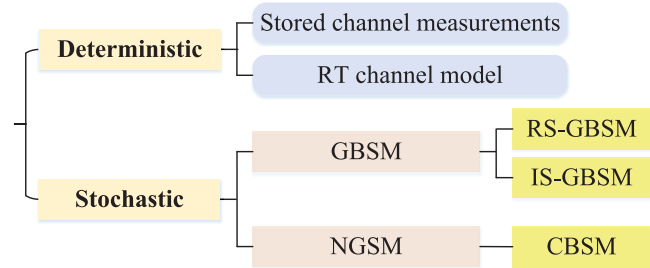


Fig. 3. Deterministic versus stochastic classification methods [23].

acquire relative parameters or the channel matrix. It is worth mentioning that GBSMs are subdivided into regular shaped (RS) which assumes that scatterers are distributed on a regular geometry, and irregular-shaped (IS) which assumes the scatterers are distributed on an irregular geometry. For 2-D RS-GBSM, one-ring, two-ring, and ellipses are usually used to mimic the scatterer distribution. For 3-D RS-GBSM, two-sphere, ellipsoids, and multiple confocal elliptic-cylinder can be applied. Twin-cluster is extensively used for IS-GBSM, which is very convenient and flexible to describe new massive MIMO properties, such as cluster birth–death (BD) and spatial nonstationarity. Details about the twin-cluster model will be introduced in Section III. In addition, NGSMs mainly indicate CBSMs.

This classification method provides an unambiguous classification of channel models. However, it should be further updated to follow the latest development of wireless channel modeling.

C. Predictive Versus Nonpredictive Channel Model Classification

We propose a unified predictive versus nonpredictive channel model classification framework, as shown in Fig. 4. This classification method aims to:

- 1) provide a more coherent classification methodology by inheriting the merit of deterministic versus stochastic method;
- 2) incorporate most existing massive MIMO channel models for completer summarization;
- 3) provide nonoverlapping and exclusive classification of various channel models.

The principles inherent in this classification framework include three consecutive layers. First, with the inclusion of AI/ML algorithms to expedite and simplify the channel modeling process, wireless channel models can be split into AI/ML-based predictive models and classical nonpredictive models. Based on extensive channel measurements and simulations at different communication scenarios with different system configurations, if the channel parameters/characteristics for an unknown channel are predicted using neural network (NN) or other AI/ML algorithms, this model belongs to AI/ML-based predictive models [54]. Otherwise, it belongs to nonpredictive models. The employed AI/ML algorithms can be further split into supervised learning, unsupervised learning, and reinforcement learning, more details can

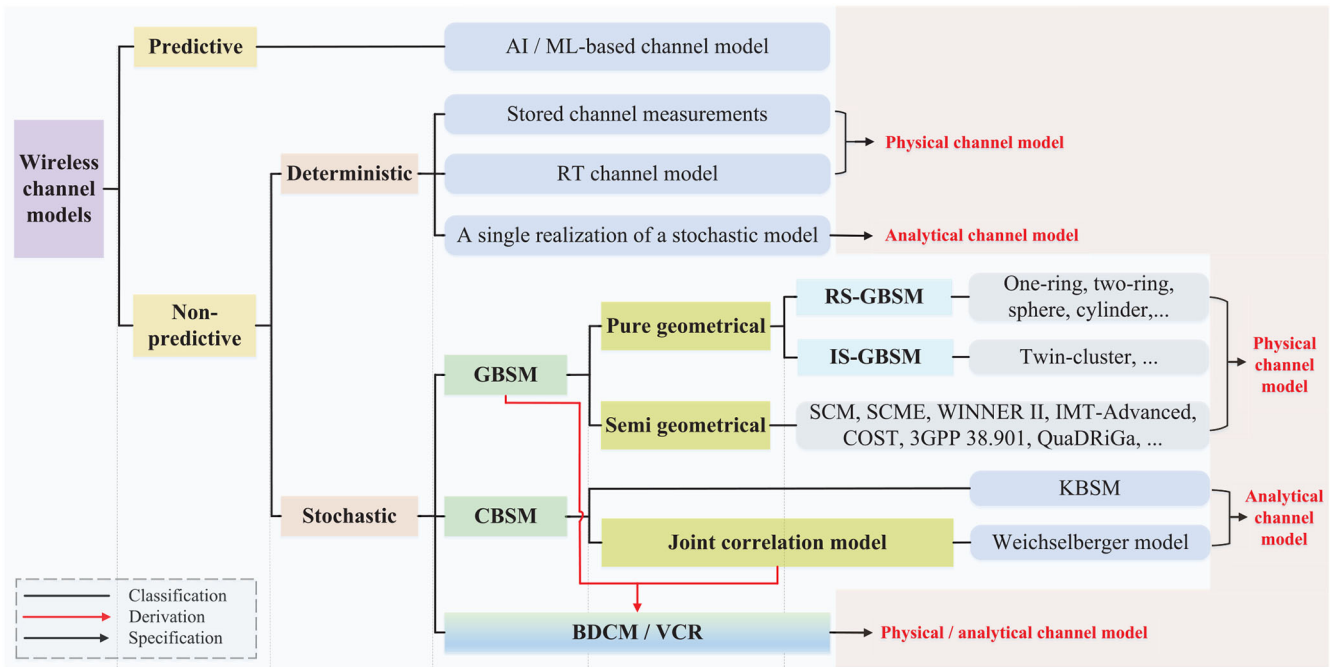


Fig. 4. Proposed classification method of wireless channel models.

be found in [55]. Second, nonpredictive channel models are classified into deterministic and stochastic models. The main criterion is similar to the above deterministic versus stochastic classification method. Third, deterministic and stochastic channel models are further split according to that channel parameters are physically or analytically motivated, respectively. For deterministic channel models, the stored channel measurements and RT channel model are physically based, while a single realization of a stochastic model belongs to analytically based. For stochastic channel models, GBSMs are physically based and CBSMs are analytically based. It is worth noting that we isolate BDCMs from CBSMs, as BDCMs are intermediate method originating from GBSMs to provide closed expressions and reduced complexity as CBSMs inherently. Here, we also categorize GBSMs as semi geometrical models, such as SCM, SCME, WINNER II/+, COST 2100, IMT-Advanced, 3GPP TR 38.901, and QuaDRiGa, and pure geometrical models which can be further separated into RS-GBSMs and IS-GBSMs. The twin-cluster model is typical for IS-GBSMs. In addition, CBSMs include the general correlated KBSM and mutual coupling-based WM. Noting that the SV, i.i.d. Rayleigh, and some hybrid channel models, such as map-based model, are not listed in this figure.

III. FUNDAMENTALS AND RECENT ADVANCES OF MASSIVE MIMO CHANNEL MODELS

In massive MIMO channels, new channel propagation characteristics are introduced by the usage of large antenna array. Therefore, conventional MIMO channel models are unable to provide accurate and computational efficient description of massive MIMO channels. In this section, we will start with a brief summary of massive MIMO channel measurements

and analyses of new channel characteristics. Then, fundamentals of various MIMO channel models and recent advances of massive MIMO channel modeling will be presented.

A. Massive MIMO Channel Characteristics

With the increase number of antenna elements, array dimension can become very large especially at the lower frequency band. Massive MIMO channels may exhibit some new channel propagation characteristics [49], [56], [57]. For example, the calculated Rayleigh distance is larger than that using conventional MIMO. MPCs impinging at the Rx or scatterers within the Rayleigh distance should be treated as the spherical wavefront. The delays, angles, and amplitudes of MPCs can change along the array. Except that, different antenna elements may see different clusters and they experience cluster BD phenomenon, or in other words, clusters have different visibility regions (VRs). This is called spatial nonstationary property. In the multiuser case, channels among different users tend to show orthogonality and the variations of channel gain decrease with the increased number of antennas, i.e., channel hardening. To validate such conjectures, some massive MIMO measurement trials have been conducted. In Table II, advanced channel measurement campaigns and corresponding analyses are summarized.

In [58], stationarities of small scale fading parameters were investigated over a large array in a LoS stadium scenario at two frequency bands. It was found that nonstationarity over ULA appears at low-frequency bands, but not necessarily at high frequency bands. Channel measurements in [59], at 2.6 GHz with 128-port virtual ULA and practical UCA in O2O, showed that PAP varies significantly along the large ULA, while UCA experiences only a small part of channels seen by ULA. In the multiuser case, ULA can provide better spatial resolution

TABLE II
MASSIVE MIMO CHANNEL CHARACTERISTICS BASED ON MEASUREMENT CAMPAIGNS

Ref.	Frequency (GHz)	Bandwidth	Scenario	Array configuration	Statistics	Channel characteristics
[58]	1.4725, 4.45	91 MHz, 100 MHz	Stadium	Tx: 128 virtual ULA	Channel coefficient, Ricean K -factor, RMS DS	Spatial non-stationarity
[59]	2.6	50 MHz	O2O	Tx: 128 virtual ULA, 128 UCA	PAP, SVS, Capacity	Spatial non-stationarity, favorable propagation
[60]	2.6	50 MHz	Court yard	Rx: 128 virtual ULA	K , PAP, antenna correlation, eigenvalue distribution	Spatial non-stationarity, near-field effect, favorable propagation
[6], [61]	2.6	40 MHz	Indoor, outdoor	Rx: 128 cylindrical	Channel gain	Channel hardening
[62]	3.33	100 MHz	Outdoor campus	Tx: 64 virtual ULA	PDP, PAP, RMS DS, RMS AS	Spatial non-stationarity
[63]	3.5	200 MHz	UMa	Tx: 256 virtual UPA Rx: 16 ODA	PAP, AAoA, AAoD, cluster number, VR	Spatial non-stationarity
[64], [65]	3.5	160 MHz	Suburban road	Tx: 8×8 planar patch Rx: 8×8 cylindrical patch	PDP, K , RMS DS	Spatial non-stationarity
[66]	5.15	–	Indoor	Rx: $10 \times 10 \times 10$ virtual cube	Spherical wave coefficient	Near-field effect
[67]	6	200 MHz	Indoor hall	Tx: 64 virtual ULA Rx: 4 virtual ULA	PADP, RMS DS, RMS AS, SCCF, quasi-stationary distance	Spatial non-stationarity
[68]	11	200 MHz	Indoor hotspot	Tx: 4×64 virtual UPA	Observed cluster length, MPC length	Spatial non-stationarity
[69]	11	160 MHz	Indoor lobby	Rx: 4×64 , 64×4 virtual UPAs	PAP	Spatial non-stationarity, near-field effect
[70], [71]	11	200 MHz	Indoor theater	Tx: 4×64 virtual UPA	RMS DS, coherent bandwidth	Spatial non-stationarity
[72]	15	4 GHz	Outdoor	Rx: 40×40 virtual UPA	K , RMS DS, RMS AAS, RMS EAS	Spatial non-stationarity
[73]	15	4 GHz	Outdoor rooftop	Rx: 40×40 UPA	PDP, PAP, RMS DS	Near-field effect
[74]	28	4 GHz	Indoor lab	Tx: 21×21 virtual UPA	PADP, RMS DS, RMS AS	Spatial non-stationarity
[75]	11, 16, 28, 38	2 GHz, 4 GHz	Indoor office	Rx: 51×51 virtual UPA, 76×76 virtual UPA, 91×91 virtual UPA, 121×121 virtual UPA	PDP, PAP, RMS DS, RMS AS, SCCF	Spatial non-stationarity, near-field effect
[76]	94	3 GHz	Indoor office	Tx: 4 virtual ULA Rx: 50×50 virtual UPA	PDP, condition number	Favorable propagation

ULA: uniform linear array; O2O: outdoor-to-outdoor; UCA: uniform circular array; PAP: power angle profile; SVS: singular value spread; AAS/EAS: azimuth/elevation angle spread; PDP: power delay profile; UPA: uniform planar array; ODA: omni-directional array; PADP: power angle delay profile; SCCF: spatial cross-correlation function.

than UCA due to larger angular resolution. In [62], [69], and [70], measurement results showed that channel nonstationarity occurs in both spatial and delay domains. In [67], channel measurements were carried out at 6 GHz for massive MIMO in an indoor hall scenario. Spatial variation along a large array was investigated. It was found that spatial variation in the NLoS case is more distinct than that in the LoS case. In [72], the 40×40 Rx virtual UPA was split into seven subarrays and measurement data was processed using the SAGE algorithm separately. Thus, parameter variations along different subarrays were observed. Statistics including the Ricean K -factor, RMS DS, AAoA, and EAoA were investigated. In addition, the concept of spatial stationary clusters was proposed by identifying multipath clusters across the array. Cluster BD along the array can be observed based on the life distances of clusters in azimuth and elevation directions. In [68], MPCs were extracted using the SAGE algorithm with a sliding window and clustered

applying a hybrid processing scheme. The BD of clusters and MPCs was statistically characterized, and a cluster-based channel model was proposed. Based on the shooting and bouncing ray (SBR) method, simulations were conducted at 15 GHz using 40×40 UPA in [73]. By analyzing PDP, PAP, and RMS DS, the near-field effect was discussed.

For multiuser communications, channel hardening and favorable propagation are desired properties in massive MIMO systems [77]. In [6], based on theory, measurement, and simulation analyses, it was pointed out that channel hardening can greatly improve reliability in massive MIMO wireless systems. The simulations were based on the COST 2100 model and its extension. In [78], an overview of massive MIMO channel characteristics was given, including the near-field effect, nonstationarity, favorable propagation conditions, and channel hardening. Such phenomena were verified by condition number and RMS DS variations calculated based on channel

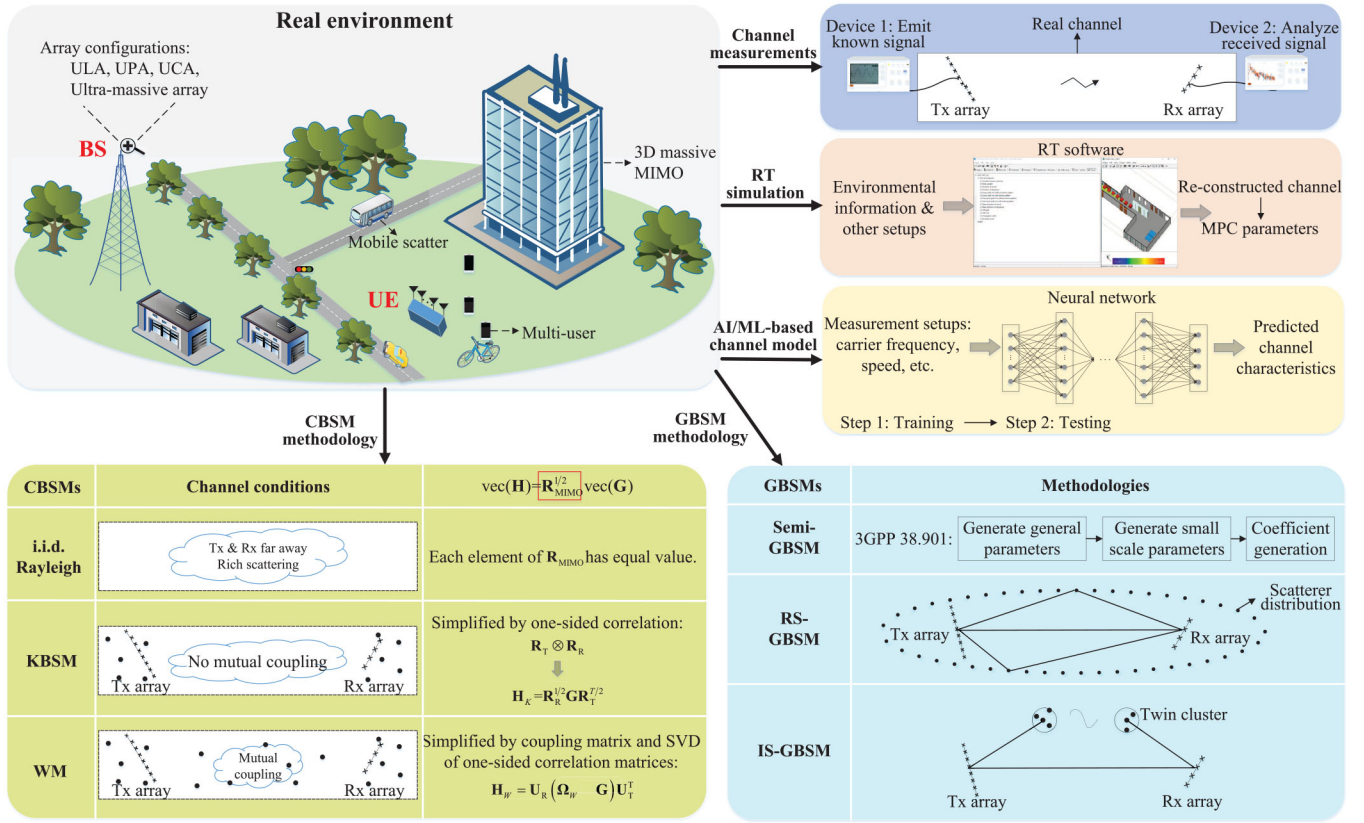


Fig. 5. Massive MIMO communication environment and abstracted channel models.

measurements in an indoor environment. More references can be found in Table II.

In general, spatial nonstationarity, near-field effect, as well as channel hardening have been found in massive MIMO channels. However, it should be noticed that existing massive MIMO channel measurements mainly centering at low-frequency bands, the massive arrays used are mostly virtually configured. Channel measurements at different frequency bands with large practical antenna array under different array configurations should be carried out, thus to provide a more convincing thorough analysis of new channel characteristics.

B. AI/ML-Based Predictive Channel Model

A description of massive MIMO wireless communication scenario is shown in Fig. 5, including the visualization and comparison of different channel modeling methodologies. In this figure, scatterers are illustrated by solid dark circles. To summarize recent advances in massive MIMO channel modeling, a survey of existing massive MIMO channel models is summarized in Table III.

Benefit from the capability of AI/ML algorithms in nonlinear data processing and prediction, they provide alternative method to generate a pervasive model for future wireless channels. In [79], a PCA-based complex-value MIMO channel modeling methodology was proposed. By comparing with 32×56 indoor measurement data, the correctness of the proposed model was validated. It was also pointed out that the proposed methodology can be used to massive MIMO

channel modeling as it is robust with the increase of antennas. In [80], an ANN-based channel model was proposed to output six channel statistical properties. The data sets were collected from real mmWave indoor channel measurement and GBSM simulations. A thorough summary of AI/ML algorithms for channel modeling can be found in [81].

However, in massive MIMO channels, AI/ML algorithms are mostly used for channel estimation for time-division duplex and frequency-division duplex, localization, beamforming, and beamsteering. In [114], the utilizations of deep learning to massive MIMO channels were reviewed, including beam selection, antenna selection, and channel estimation. In [115], two NN-based models were developed for time-varying mmWave MIMO channels, considering both large-scale and small-scale fading. They were testified by channel measurements at 26 GHz in an outdoor microcell and compared to GBSM cluster-based MIMO channel model. In [116], an efficient channel estimation scheme was proposed to address spherical-wave features in THz ultramassive MIMO systems. It can be seen that there are still many works to be done for massive MIMO channel modeling employing AI/ML algorithms.

C. Deterministic Channel Model

Three ways to obtain fixed MPC parameters for deterministic channel models are channel measurements, RT simulations, and realizations of stochastic models. Using either a time-domain channel sounder or frequency-domain vector network

TABLE III
RECENT ADVANCES IN MASSIVE MIMO CHANNEL MODELING

Ref.	Model	Year	Frequency (GHz)	Array configuration	Scenario	Statistics
[79]	AI/ML-based predictive (PCA)	2020	3.5	32×56 UPA	Indoor meeting room	Channel capacity
[80]	AI/ML-based predictive (ANN)	2020	11, 16, 28, 38	51×51 UPA, 76×76 UPA, 91×91 UPA, 121×121 UPA	Indoor office	Received power, RMS DS, RMS AS
[82]	Channel measurement	2018	2.53	Cylindrical arrays	UMa	Intra-/inter-cluster parameters
[83]	RT	2017	26	$64/1024$ ULA, 128 UPA	Indoor	PL, SF, RMS DS, coherence bandwidth
[84]	RT	2017	5.25, 10.1, 28-30	25 UPA	Urban outdoor	PL, PAP, channel capacity
[85]	RT	2017	28	64 ULA	Indoor	PDP, PAAP
[86]	RT	2019	26	64 ULA	Indoor center hall	PDP, PAAP, PAEP
[87]	KBSM	2015	–	64×64 ULA	–	SCCF, channel capacity
[88]	WM	2016	–	ULA	–	Channel capacity
[89]	WM	2019	–	ULA	Multi-user	Channel hardening, favorable propagation
[4], [90]	WM	2019, 2020	–	ULA	Multi-user, LoS, indoor	SE
[91]	Semi geometrical (COST 2100)	2013	2.6	128 virtual ULA	Semi-urban outdoor	BS-VR
[92]	Semi geometrical (QuaDRiGa)	2016	–	64 ULA	Indoor	Multi-user consistency, spatial non-stationary, spherical wavefront
[93]	Semi geometrical (3GPP 3D)	2019	2	ULA	UMa, RMa, UMi street canyon	Spatial consistency
[94]	Semi geometrical (COST 2100)	2020	2.6	128 virtual ULA	Outdoor	BS-VR, MPC-VR
[95]	Semi geometrical (COST 2100)	2021	2.605	32 ULA, UPA	–	PDP, PAP
[96]	RS-GBSM (Two-cylinder)	2015	2, 28	Any array (4 ULA)	200 m apart	ACF, SCCF, Doppler PSD, condition number
[97]	RS-GBSM (Multi-ring)	2016	–	ULA	–	Cluster VR length, cluster power variation
[98], [99]	RS-GBSM (Multi-confocal ellipsoid)	2018, 2019	2	(32×32) UPAs	Mobile	TACF, SCCF
[100]	RS-GBSM (One-ring, ellipse), Semi geometrical	2020	2	Any array (100 ULA)	NLoS, 100 m apart	TACF, PSD, SCCF, FCF
[101]	RS-GBSM (Two-ring, semi-ellipsoidal)	2020	2	10 ULA	Cell free	TACF, SCCF, stationary interval
[102]	RS-GBSM	2020	VLC	–	VLC	Received power
[103]	RS-GBSM	2020	–	ULA	V2V	S-T-F CF
[104]	IS-GBSM	2015	–	32×32 ULAs	–	SCCF
[105]	IS-GBSM	2018	2, 2.6	100/128 ULA	–	TACF, SCCF, cluster VR length
[106]	IS-GBSM	2021	2.6	128 ULA	–	SCCF, cluster VR length, cluster power variation
[107]	IS-GBSM	2021	–	ULA	RIS	TACF, SCCF
[108]	IS-GBSM	2021	–	UPA	THz	S-T-F CF, RMS DS, RMS AS
[110]	IS-GBSM	2021	sub-6, mmWave	–	UAV, maritime	TACF, SCCF, PSD, RMS DS, stationary interval
[111]	IS-GBSM	2021	mmWave	ULA	UAV	PDP, TACF, SCCF, RMS DS
[112]	IS-GBSM	2022	mmWave	UPA	IoT	Channel estimation
[28], [113]	BDCM	2021, 2017	–	128 ULA	Multi-user	Secret key rate, per beam synchronization

PCA: principal component analysis; ANN: artificial neural networks; UMa: urban macrocell; RMa: rural macrocell; UMi: urban microcell; TACF: Temporal autocorrelation function; PSD: power spectral density; RIS: reconfigurable intelligent surface; S-T-F: space-time-frequency.

analyzer, channel measurements can be carried out at different environments using different setups. After high-resolution data processing using such as the SAGE algorithm, detailed channel

parameters can be estimated. The constructed CIR/CTF can be validated using measurement data and provide accurate characterization of certain wireless channels. Related channel

measurement campaigns can be found in Table II. RT can be used to replace channel measurements, thus to reduce both economy and time costs [117]. There are many kinds of RT softwares [16], including Wireless Insite, CloudRT, RadioTracer, WinProp, and CrossWave. To reduce the computation time using RT and uniform theory of diffraction (UTD), efficient acceleration techniques were proposed, such as ray tubes [118]. In [119], the proposed ray launching scheme was compared with urban channel measurement data at 890 MHz. This work is one of the first group papers to use RT for radio-mobile propagation. By inputting necessary environment descriptions and system configurations, RT can be used to trace every ray. Parameters of each ray can be computed based on UTD [120]. In [121], the importance of RT in future channel modeling was emphasized. It was pointed out that with the accurate positioning systems, RT can not only be used “offline” but also can be embedded into future systems “online” to provide real-time channel prediction. More RT simulations for massive MIMO channels with different array configurations, frequency bands, and scenarios can be found in Table III. Though RT can provide accurate channel description for a given environment with crucial physical parameters, the accuracy is very much relying on the full description of the communication environment. Besides, both channel measurements and RT are complex and site specific, it is impossible to traverse all communication scenarios. A single realization of a stochastic channel model is actually a sample function with certain parameters. Especially, for ergodic stochastic process, statistical properties of any sample function can represent that of the ergodic stochastic model.

D. CBSM

Let us consider a time-invariant massive MIMO system with N_T transmit and N_R receive antennas. Both Tx and Rx are equipped with ULAs. The complete channel model can be given as follows:

$$\mathbf{H}_{\text{Total}} = \mathbf{Q}\mathbf{H} \quad (1)$$

where \mathbf{Q} is a large-scale coefficient and $\mathbf{Q} = (PL \cdot SD \cdot BL \cdot OL)^{1/2}$, with PL denoting the path loss caused by the propagation distance. SD is the shadow fading which can be modeled as lognormal distributed, BL is the blockage effect caused by humans and vehicles [122], and OL is the oxygen absorption loss exhibits in high-frequency bands communications. In this article, the subscripts \cdot_T and \cdot_R indicate entity at the Tx and Rx sides, respectively. The distances between adjacent antennas are δ_T and δ_R for the Tx and Rx, respectively. In this section, the NLoS case and small-scale fading are considered. The channel matrix \mathbf{H} can be expressed as follows:

$$\mathbf{H} = \begin{bmatrix} h_{1,1} & \cdots & h_{1,N_T} \\ \vdots & \ddots & \vdots \\ h_{N_R,1} & \cdots & h_{N_R,N_T} \end{bmatrix}. \quad (2)$$

The matrix dimension is $N_R \times N_T$, where $h_{q,p}$ denotes the CIR of the q th Rx antenna and the p th Tx antenna. The same principles can be followed for each delay tap, thus to acquire the wideband channel models.

If the channel coefficient is assumed as zero-mean complex Gaussian distributed, the CIR is completely determined by the channel covariance matrix only and can be generalized as [123]

$$\text{vec}(\mathbf{H}) = \mathbf{R}_{\text{MIMO}}^{1/2} \text{vec}(\mathbf{G}) \quad (3)$$

where $\text{vec}(\cdot)$ is the vectorization of matrix, it stacks the columns of \mathbf{H} into a column vector of size $N_R N_T \times 1$, and $\text{vec}(\mathbf{G})$ is an i.i.d. zero mean and unit variance vector. It should be noted that \mathbf{R}_{MIMO} is the full correlation matrix. It describes the inherent spatial structure of the massive MIMO channel and contains the mutual correlation values among all channel matrix elements. It can be calculated using symmetric channel-oriented way and asymmetric link-end-oriented way [124]. The former way is mostly used as it forms a Hermitian matrix

$$\mathbf{R}_{\text{MIMO}} = E\{\text{vec}(\mathbf{H})\text{vec}^H(\mathbf{H})\} \quad (4)$$

where $E\{\cdot\}$ is the expectation operator and $(\cdot)^H$ is the conjugate transpose. The size of \mathbf{R}_{MIMO} is $N_R N_T \times N_R N_T$. One dimension has the same number of elements as the channel matrix, that is why it is called channel oriented. Each sequentially N_R diagonal elements of \mathbf{R}_{MIMO} are spatial correlations from the same Tx antenna. It can be seen that \mathbf{R}_{MIMO} contains $N_R^2 N_T^2$ elements in total. In order to reduce the huge size of \mathbf{R}_{MIMO} in calculating $\text{vec}(\mathbf{H})$, the following models were proposed successively.

1) *i.i.d. Rayleigh Channel Model*: The i.i.d. Rayleigh model assumes no correlation and mutual coupling between transmit or receive antennas. The elements of fast fading channel matrix are i.i.d. Gaussian random variables. Elements of the full correlation matrix are equal to one certain value. This model can only be used when the MPCs are rich and distributed uniformly in the spatial domain.

2) *KBSM*: KBSM was proposed in 1998 by Chuah *et al.* [125]. It assumes that correlation at the Tx is independent from the correlation at the Rx. This implies that nearly no scatterers exist between the Tx and Rx. All AoAs and AoDs are deemed to be completely independent, which is over idealistic. But due to the simplicity of KBSM, it is popularly used in massive MIMO channels.

The total correlation of the channel can be expressed as the Kronecker product of the correlation matrices at the Tx and the Rx [125]

$$\mathbf{R}_K = \mathbf{R}_T \otimes \mathbf{R}_R \quad (5)$$

where $\mathbf{R}_T = E\{\mathbf{H}^T \mathbf{H}^*\}$ and $\mathbf{R}_R = E\{\mathbf{H}\mathbf{H}^H\}$ are also called the one-sided correlation matrices. Consequently, KBSM is expressed as

$$\mathbf{H}_K = \mathbf{R}_R^{1/2} \mathbf{G} \mathbf{R}_T^{T/2}. \quad (6)$$

Operating singular value decomposition for \mathbf{R}_T and \mathbf{R}_R

$$\mathbf{R} = \mathbf{U}_T \mathbf{\Lambda}_T \mathbf{U}_T^H \quad (7)$$

and

$$\mathbf{R}_R = \mathbf{U}_R \mathbf{\Lambda}_R \mathbf{U}_R^H \quad (8)$$

with \mathbf{U}_T and \mathbf{U}_R are eigenbases consisting of the eigenvectors denoted by $\mathbf{u}_{T,n}$ and $\mathbf{u}_{R,m}$, respectively. It is also noted that

Λ_T and Λ_R are diagonal matrices containing the eigenvalues of $\tilde{\mathbf{R}}_T$ and $\tilde{\mathbf{R}}_R$, respectively. Here, we also denote vectors $\tilde{\lambda}_T$ and $\tilde{\lambda}_R$ to consist of the square root of the eigenvalues of $\tilde{\mathbf{R}}_T$ and $\tilde{\mathbf{R}}_R$, respectively. Thus, (6) can be equivalently formulated as

$$\mathbf{H}_K = \mathbf{U}_R \left((\tilde{\lambda}_R \tilde{\lambda}_T^T) \odot \mathbf{G} \right) \mathbf{U}_T^T. \quad (9)$$

To incorporate new characteristics of massive MIMO channels, in [87], KBSM was extended for massive MIMO channels. It used the BD process to incorporate evolution of scatterer sets on the array axis. Channel capacities in both the high and low signal-to-noise ratio (SNR) regimes were derived. Taking the Tx side as an example, the survival probability of scatterers from the p th antenna to the p' th antenna was defined as [87]

$$E_{T,pp'} = e^{-\beta|p-p'|} \quad (10)$$

where $p, p' = 1, \dots, N_T$ and β describe how fast a scatterer disappears on the Tx array axis. $\mathbf{E}_T = [E_{T,pp'}]_{N_T \times N_T}$ denotes the survival matrix at the Tx side. Similarly, $\mathbf{E}_R = [E_{R,qq'}]_{N_R \times N_R}$ denotes the survival matrix at the Rx side ($q, q' = 1, \dots, N_R$), the proposed KBSM-BD-AA was expressed as

$$\tilde{\mathbf{H}}_K = (\mathbf{E}_R \circ \mathbf{R}_R)^{1/2} \mathbf{G} (\mathbf{E}_T \circ \mathbf{R}_T)^{T/2} \quad (11)$$

with \circ denotes the Hadamard product.

Other works have been done for massive MIMO channels using KBSM. For example, in [126], KBSM was used to analyze the achievable SE of massive MIMO with multi-antenna users. In [127], antenna selection was studied for massive MIMO channels by considering KBSM using PCA. It was found that KBSM can underestimate channel capacity. This drawback may become more severe in massive MIMO channels. Because more scatterers can be resolved, spatial correlations at both link ends are not isolated [128].

3) *WM*: WM was proposed in 2003 by Weichselberger *et al.* [129]. It takes account of joint correlation properties by using the average coupling between the eigenvectors of both ends. Different from the KBSM, WM does not divide the channel spatial correlation properties into two separate Tx and Rx contributions. It can not only alleviate the restriction imposed by KBSM and describe the joint spatial structure of the channel but also alleviate the restriction imposed by BDCM and adopts the spatial eigenbases to the array configuration. It includes both KBSM and BDCM as special cases and can be applied to any array configuration and any scenario. WM can be written as [129]

$$\mathbf{H}_W = \mathbf{U}_R (\tilde{\mathbf{\Omega}}_W \odot \mathbf{G}) \mathbf{U}_T^T \quad (12)$$

where $\tilde{\mathbf{\Omega}}_W$ has full rank and consists of real-valued nonnegative elements. It links the correlation properties of both ends. It is the average energy of the virtual single-input–single-output (SISO) channel between each eigenmode of the Tx side and each eigenmode of the Rx side. It can be calculated as the elementwise square root of the coupling matrix given by [129]

$$\mathbf{\Omega}_W = E \{ (\mathbf{u}_R^H \mathbf{H} \mathbf{u}_T^*) \odot (\mathbf{u}_R^T \mathbf{H}^* \mathbf{u}_T) \}. \quad (13)$$

The elements in the q th row and p th column of $\mathbf{\Omega}_W$ can be calculated as

$$\begin{aligned} [\mathbf{\Omega}_W]_{q,p} &= \omega_{q,p} = E \left\{ \left| \mathbf{u}_{R,q}^H \mathbf{H} \mathbf{u}_{T,p} \right|^2 \right\} \\ &= (\mathbf{u}_{T,p} \otimes \mathbf{u}_{R,q})^H \mathbf{R}_{\text{MIMO}} (\mathbf{u}_{T,p} \otimes \mathbf{u}_{R,q}). \end{aligned} \quad (14)$$

The reason we call $\mathbf{\Omega}_W$ as a coupling matrix is that its coefficients specify the mean amount of energy that is coupled from the m th eigenvector of the Tx side to the n th eigenvector of the Rx side, and *vice versa*. It reflects the spatial arrangement of scattering objects.

There are only few papers about massive MIMO WM. In [89], analysis of multiuser massive MIMO performance regarding channel hardening and favorable propagation was carried out based on WM. In [88], WM was extended to 3-D and a novel coupling mode was proposed based on WINNER II. System capacity with equal power allocation was analyzed. It was shown that the proposed 3-D WM was more accurate than 3-D KBSM in capacity analysis. As pointed out in [129], $\mathbf{\Omega}$ can influence channel capacity and can be used to determine whether spatial multiplexing or diversity to be employed. In [90], WM was employed for LoS propagation of multi-antenna user massive MIMO channel under jointly correlated Ricean fading. The uplink SE was further derived with a rigorous closed-form expression. In [130], the channel matrix for massive MIMO channel was divided into fixed part for LoS component and random part for NLoS components. For the random matrix, it extended WM by using experimental distributions based on measurement data for amplitude and phase of the coupling matrix. The channel capacity and SVS were compared among measurement data, KBSM, WM, and the proposed model. It was shown that the proposed model fitted well with measurement data and performed better than traditional WM. That is because the coupling matrix in traditional WM is generated from theoretical analysis and without real measurement validation.

E. GBSM

Different from CBSMs, GBSMs are more accurate and flexible to describe wireless channels. This kind of model provides a general equation with many channel model parameters, which are derived based on the geometrical relationships and experimental distributions. For RS-GBSM, the following GBSMs are popularly used.

- 1) *One-Ring Model*: Scatterers are distributed on a circle with the center being Rx (mobile station). It is usually used for the macrocell narrowband channels, where the Tx and Rx are far away with the Tx is highly elevated and unobstructed.
- 2) *Two-Ring Model*: Scatterers are distributed on two circles with the center being the Tx and Rx, respectively. It is used in microcell scenarios, where the Tx and Rx are far away with the contribution of remote scatterers to the total received power are neglected.
- 3) *Ellipse Model*: The ellipse defines the geometrical distribution of the scatterers with foci at the center of Tx and Rx arrays. For one ellipse, the time of arrival is a

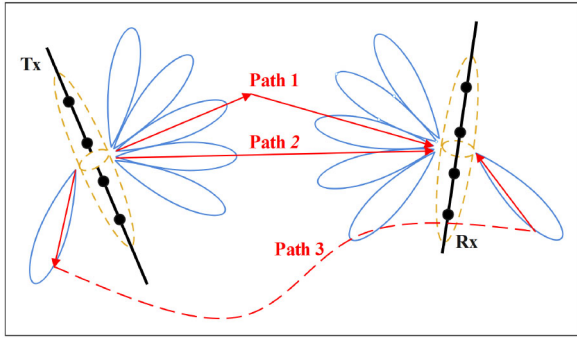


Fig. 7. Signal transmission in the beam domain.

3-D general THz IS-GBSM was proposed to describe the non-stationarities and cluster evolution in S-T-F domains. There are also newly proposed GBMSs for UAV and maritime scenarios [109], [110]. In [96], a 3-D two cylinder RS-GBSM was proposed by incorporating spherical wavefront and nonstationary property. By comparing with the 3GPP 3-D MIMO model, the correctness of the proposed model was verified.

F. BDCM

VCR was proposed in 2000 by Sayeed by utilizing a virtual partitioning of the spatial domain to characterize MIMO channels [29], [133]. This model was further developed for massive MIMO channels in recent years, but usually known as BDCM. For clarity, we unify the designations of these two models as BDCM.

BDCM is a method originated from beamforming, or we can see BDCM adds a beamform preprocessor compared with array domain channel modeling. In this way, advantages can be obtained, such as reduced computational complexity, decreased sensitivity to array imperfections, and lower SNR resolution thresholds. This method can be regarded as a rising solution to cope with the increasing complexity of massive MIMO channel modeling. As most channel models are nonlinear in spatial angles, they are usually difficult to be incorporated in transceiver design and capacity computations. However, BDCM keeps the essence of GBMSs and provides a tractable channel characterization [134], [135].

In traditional array domain, signals emitted from and received at a certain pair of antenna elements from all directions of the 3-D space. Then, the CIR is the summation of multipaths contributions. In the beam domain, the 2-D space at the Tx (Rx) side is divided into several sectors and the beam-domain channel can separate paths of different angles by different beams [27]. Different elements of the channel matrix represent signals from different transmit and receive angles. The CIR of one certain pair of sectors is the summation of multipaths originated and fallen at this pair of beam sectors, see Fig. 7. Relations between the virtual beamspace channel representation \mathbf{H}_B and \mathbf{H} is [29]

$$\mathbf{H}_B = \mathbf{A}_R^H \mathbf{H} \mathbf{A}_T \quad (18)$$

where \mathbf{A}_T and \mathbf{A}_R are unitary matrices, $\mathbf{A}_R^H \mathbf{A}_R = \mathbf{I}$ and $\mathbf{A}_T^H \mathbf{A}_T = \mathbf{I}$. The columns are orthogonal steering vectors determined by the angle of sectors. Taking ULA as an example, if

M sectors are formed, we can denote \mathbf{A}_T and \mathbf{A}_R as

$$\mathbf{A}_R = \frac{1}{\sqrt{N_R}} [\mathbf{c}_R(\theta_{R,1}), \dots, \mathbf{c}_R(\theta_{R,N_R})] \quad (19a)$$

and

$$\mathbf{A}_T = \frac{1}{\sqrt{N_T}} [\mathbf{c}_T(\theta_{T,1}), \dots, \mathbf{c}_T(\theta_{T,N_T})] \quad (19b)$$

with $\theta_{R,1}, \dots, \theta_{R,N_R}$ and $\theta_{T,1}, \dots, \theta_{T,N_T}$ are the sampling angles at the Tx side and the Rx side, respectively. In addition,

$$\mathbf{c}_R(\theta_{R,n_R}) = \left[1, \dots, e^{-j\frac{2\pi}{\lambda}(N_R-1)d_R \sin(\theta_{R,n_R})} \right]^T \quad (20a)$$

and

$$\mathbf{c}_T(\theta_{T,n_T}) = \left[1, \dots, e^{-j\frac{2\pi}{\lambda}(N_T-1)d_T \sin(\theta_{T,n_T})} \right]^T \quad (20b)$$

where $n_R = 1, \dots, N_R$ and $n_T = 1, \dots, N_T$.

The BDCM can also be represented as [29]

$$\mathbf{H}_B = \mathbf{A}_R (\tilde{\mathbf{\Omega}}_B \odot \mathbf{G}) \mathbf{A}_T^H \quad (21)$$

where $\tilde{\mathbf{\Omega}}_B$ is elementwise square root of the power coupling matrix $\mathbf{\Omega}_B$

$$\mathbf{\Omega}_B = E \{ (\mathbf{A}_R^H \mathbf{H} \mathbf{A}_T^*) \odot (\mathbf{A}_R^T \mathbf{H}^* \mathbf{A}_T) \} \quad (22)$$

whose positive and real-valued elements determine the average power-coupling between the q th transmit and the p th receive virtual directions. The unitary matrices are used to forming virtual beamspace and the coupling matrix is the average power between different beam pairs. BDCM operates DFT with fixed virtual angles determined by the spatial resolution of the arrays. It was specified in [136] that when the antenna numbers of the Tx and Rx ULAs grow large, the eigenspaces of one-sided matrices can be approximated by unitary DFT matrices. Under the virtual beamspace representation, \mathbf{R}_T and \mathbf{R}_R are approximately Toeplitz.

In [113], BDCM was further used in narrowband multiuser massive MIMO channel to derive and maximize the secret key rate [28]. It was also pointed out in [137] that the ability to work in a reduced dimension beamspace is even of more value in the case of a UPA since the total number of elements may be quite high. For a practical number of antenna elements, the approximation of the true eigenbases by the predefined DFT matrices can be rather poor. In [129], it was pointed out that under the division of virtual directions at both ends, the assumption of uncorrelated AoA and AoD may not hold, even though the steering vectors become very sharp with a large number of antennas. However, as the number of antenna elements goes to infinity, the DFT matrices serve as asymptotically optimal eigenfunctions for the channel matrix. As a consequence, the matrix elements of \mathbf{H} can become insignificantly correlated when BDCM is applied to massive MIMO channels. In [36], an attempt of modeling in the beam domain was made for massive MIMO channels, which transformed existing GBMSs from the antenna domain into the beam domain. Both spherical wavefront and space-time nonstationarity were considered.

It should be noted that, with the inclusion of spherical wavefront and nonstationarity, it is not easy to get the unitary

TABLE IV
COMPARISONS OF MASSIVE MIMO CHANNEL MODELS

Models	Deterministic	KBSM	RS-GBSM	IS-GBSM
WM	–	[88], [31]–[34]	–	–
Semi geometrical	[93], [37], [38], [39]	[30], [40]	[96], [100]	–
BDCM	[35]	[32], [33]	–	[36]
Hybrid	–	[33]	–	–

matrices. Another way to establish a BDCM is to directly sum the contributions of MPCs in each virtual cluster up. Problems remain are how to describe spherical wavefront and spatial nonstationarity in the beam domain, and is there any other new beam-domain channel characteristics need to be considered. By comparing with existing GBSMs, it was concluded that the proposed BDCMs have less complexity and more convenient for transmission design. Therefore, their potential in massive MIMO channel modeling needs to be further investigated.

IV. COMPARISON OF MASSIVE MIMO CHANNEL MODELS

A. Survey of Channel Model Comparison Works

There are some existing works that compare different massive MIMO channel models, as shown in Table IV. In [37], the coherence bandwidth and downlink data rate of massive MIMO channel with 256 BS antennas were investigated by using RT simulations and the WINNER II model. It was pointed out that the favorable features generated with the WINNER II model over RT was worth further investigating. For CBSMs, they are unable to capture the spatial–temporal–frequency nonstationary properties [128]. Channel modeling using KBSM and WM were introduced and compared in [31]. In [32], performances of three CBSMs were assessed via PAS, average mutual information, and average diversity measure. It is defined that a good model should render the relevant aspects of MIMO channel to be deployed. In [35], BDCM was used to represent the MIMO channel model in the angular domain from RT simulation of a SISO system. Compared with KBSM and BDCM, WM is scarcely used in massive MIMO channels on account of the increased number of parameters to be specified [89]. In [33], a general model framework of CBSMs was presented for wideband MIMO channels. Channel measurements were carried out to evaluate the joint AoA–AoD–delay power spectrum and capacity of the i.i.d. Rayleigh model, KBSM, WM, BDCM, and the hybrid model. In [138], six massive MIMO channel models were compared, including one KBSM–BD–AA and five GBSMs consisting of the 2-D elliptical model, the 2-D parabolic model, the 3-D twin-cluster model, the 3-D 5G channel model, and the 3-D ellipsoid model. It was shown that SCCFs and channel capacities of those 3-D channel models are larger than those of 2-D channel models. In [93], a GBSM for massive MIMO spatial consistency was proposed. In order to validate the behavior of the proposed model, extensive RT simulations were performed to show very good agreement [139].

It can be seen in Table IV that most works concentrate on KBSM and semi-geometrical model. Channel model comparison of massive MIMO channel models is scarce, especially in lack of comparison of ML-based and BDCM with other channel models.

B. KPIs for Evaluating Channel Models

There are mainly three KPIs to evaluate the performance of channel model, including accuracy, complexity, and pervasiveness/universality. Comparisons of classical nonpredictive channel models are illustrated in Fig. 8.

1) *Accuracy*: It indicates to what extent the real channel is reproduced. The calculated statistical property and systematical performance of the channel model should both be sufficiently accurate to represent those of the corresponding real wireless propagation channel. The commonly interested channel statistical properties consist of the first-order statistics affected by the scattering environment [mean, probability density function (PDF), and cumulative distribution function (CDF)], the second order statistics [time autocorrelation function (ACF), time/frequency/spatial cross-correlation function (CCF), Doppler/delay/angular power spectral density (PSD), envelope level crossing rate (LCR), and average fade duration (AFD)], and other high-order statistics. For instance, in order to analyze the correlation properties between different antennas, SCCF can be calculated. For GBSM, it can be calculated as

$$\begin{aligned} \rho_{qp,q'p'}(\delta_T, \delta_R) &= E \left[\frac{h_{qp}^* h_{q'p'}}{|h_{qp}^*| |h_{q'p'}|} \right] \\ &= \rho_{qp,q'p'}^{\text{LoS}}(\delta_T, \delta_R) + \rho_{qp,q'p'}^{\text{NLoS}}(\delta_T, \delta_R). \end{aligned} \quad (23)$$

Similarly, SCCFs for CBSMs can be calculated. For BDCM, the SCCF should be calculated between different beams. According to the SCCF [140], the coherence distance indicating the minimum array element spacing to maintain channel stationarity can be calculated, i.e., channel within this distance does not change significantly.

Systematic performances can be measured by channel capacity, bit error rate, etc. Considering a single-user case, without channel knowledge at the Tx side, the channel capacity with equal power allocation can be calculated as

$$C = E \left\{ \log_2 \left[\det \left(\mathbf{I} + \frac{\text{SNR}}{N_T} \bar{\mathbf{H}} \bar{\mathbf{H}}^H \right) \right] \right\} \quad (\text{bit/s/Hz}) \quad (24)$$

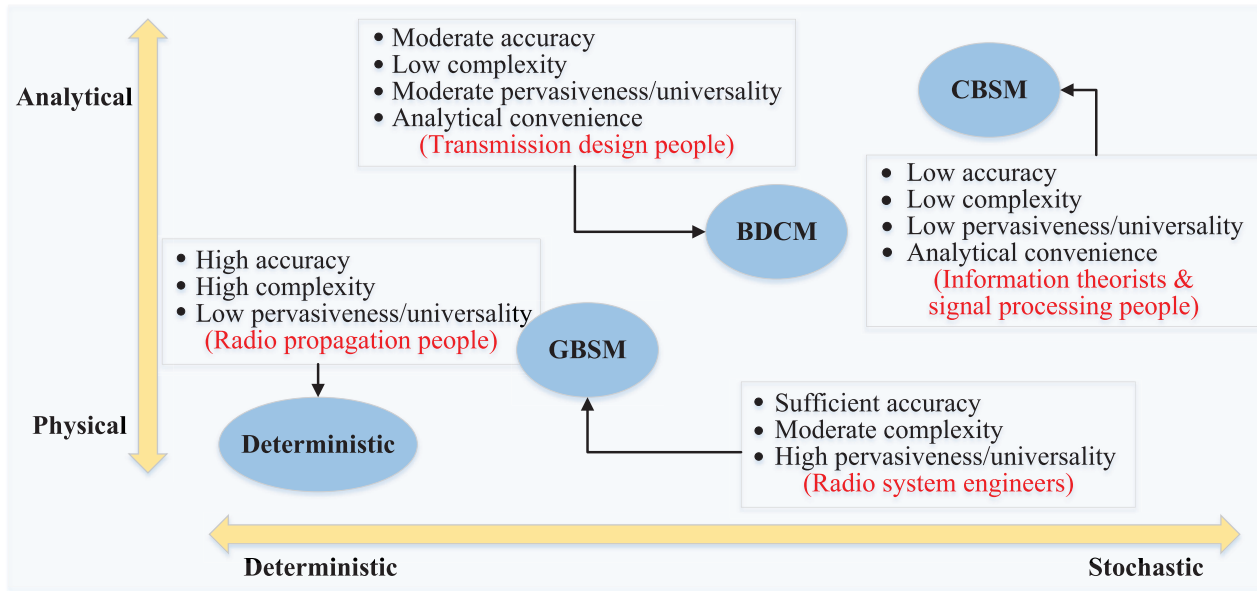


Fig. 8. Comparisons of nonpredictive channel models.

where $\det(\cdot)$ denotes the determinant operation and $\tilde{\mathbf{H}}$ is the normalized channel matrix

$$\tilde{\mathbf{H}} = \mathbf{H} \left\{ \frac{1}{N_T N_R} \sum_{q,p} |h_{q,p}|^2 \right\}^{-\frac{1}{2}}. \quad (25)$$

For KBSM-BD-AA, channel capacity can be calculated by substituting $\tilde{\mathbf{H}}$ with the normalized $\tilde{\mathbf{H}}_K$. For BDCMs, the channel number $N_T N_R$ should be replaced by the virtual beam number $M_T M_R$. Under ideal conditions, i.e., rich scattering but uncorrelated environment, the theoretical capacity increases linearly as the minimum Tx and Rx numbers. However, due to the spatial correlation, the calculated channel capacity is usually underestimated and lower than expected, especially for indoor environments. This is because the correlation properties at/between the Tx and Rx are ignored. It was shown in many literatures that KBSM has the lowest capacity than other models as it usually underestimates channel capacity. In [125], calculations of capacity with water filling and equal power allocation methods were presented.

In Fig. 9, channel capacities calculated using different channel models are illustrated and compared with real measurement data. The channel measurement is conducted in an urban environment with 32 Rx antennas and 8 Tx antennas at 5.3 GHz. The GBSM is simulated referring to [106]. It can be seen that GBSM provides the best fitting with channel measurement data, while BDCM next to it. The KBSM performs the worst as it ignores the dependencies between Tx and Rx link ends. The performances of full correlation-based model and WM are quite similar, however, the accuracies are less satisfactory.

2) *Complexity*: It measures the operations needed for channel model generation. The derivation of model parameters and the generation of the channel matrix should be labor/economic/computational efficient.

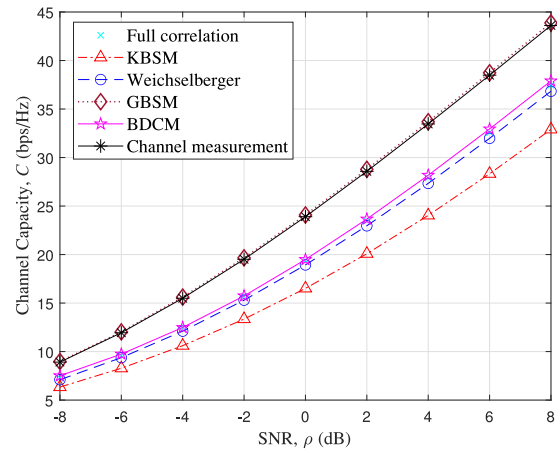


Fig. 9. Channel capacities of various channel models.

According to the methodologies to obtain different channel models, the complexity of channel models can be compared. Deterministic channel models have the highest complexity as they are site-specific, GBSMs can characterize categories of environments but have to derive parameters for each MPC, they both can provide the most accurate description of wireless channels. CBSMs have very low complexity, with KBSM having $N_T^2 + N_R^2$ and WM having $N_T N_R + N_T(N_T - 1) + N_R(N_R - 1)$. BDCM have $N_T N_R$ parameters to be determined and also have very low complexity. The AI/ML-based predictive channel models are expected to provide lower complexity than conventional nonpredictive channel models. In massive MIMO channel modeling, the complexity can be increased with array size, as well as the inclusion of new channel characteristics.

3) *Pervasiveness/Universality*: The proposed channel model should be suitable for a wide range of propagation scenarios with different system setups.

As channel measurement and RT simulation are exclusive for certain communication scenarios, they are not flexible for the characterization of different channels. CBSMs are based on the joint spatial correlation properties at Tx and Rx sides, they have the moderate pervasiveness/universality. BDCMs are intermediate method originating from GBSMs to provide closed expression and reduced complexity as CBSMs. They also have the moderate pervasiveness/universality. GBSMs, however, benefit from the usage of the geometrical distribution of scatterers, are more flexible for different scenarios. Predictive channel models should be trained with extensive measurement/simulation data and adapted to unknown channels. This guarantees their basic pervasiveness/universality.

V. FUTURE RESEARCH CHALLENGES

A. Full Exploration of Existing Channel Modeling Methods

As introduced above, there are already some works toward massive MIMO channel modeling. However, most of them are based on the GBSMs, which cannot provide the best tradeoff among three KPIs. By comparing different channel models, it can be seen that BDCMs and AI/ML-based predictive models have moderate performances. To give a better description of massive MIMO channels, these models should be further explored. Furthermore, AI/ML-based predictive channel models can be used to acquire timely prediction of wireless channels at new frequency bands and scenarios.

In order to further improve performance of massive MIMO channel models, another natural thought is to propose new channel models that flexibly incorporating the advantages of different channel models. The ultimate aim of this combination is to achieve a better tradeoff among three KPIs [23]. For example, METIS is a hybrid channel model that incorporates both a map-based model to generate large-scale parameters and a GBSM to get small scale parameters. In [141], a statistical block fading channel model was presented for multiuser massive MIMO systems. It incorporated the properties of CBSM and GBSM to simulate correlation in time/frequency domain and spatial correlation, respectively. Taking new channel characteristics of massive MIMO into consideration, how to provide a better description of massive MIMO channels based on the combination of existing channel models is worth further investigating.

B. Characterization of Multiuser (Ultra) Massive MIMO Channels

As shown in Fig. 5, 3-D and multiuser massive MIMO are promising for future wireless communication systems [142]. The impact of array dimension has also motivated ultramassive MIMO systems. The ultramassive array dimension could attain several tens of meters. It can be integrated into large structures, such as large shopping malls, that serve a large number of devices [143], [144]. In addition, with the employment of full-digital beamforming technique to acquire better massive MIMO system performance, the uplink and downlink channels

will exhibit nonreciprocal property. By facilitating with different array patterns, more users can be accessed in the uplink, while better SNR can be obtained in the downlink. Therefore, another important characteristic of massive MIMO channels is the asymmetric phenomenon. However, existing analyses of various massive MIMO channel characteristics are still not sufficient, especially in lack of comprehensive channel measurements and analyses under different array configurations. To provide accurate channel modeling, more channel measurements should be conducted and new channel characteristics should be fully investigated.

C. Pervasive Massive MIMO Channel Models at All Frequency Bands and All Scenarios

The ultimate aim of massive MIMO channel modeling is to propose pervasive channel models, which are able to characterize wireless channels at different frequency bands and all communication scenarios. Here, all frequency bands include sub-6 GHz, mmWave, THz, and optical wireless communications [145]. The pervasive channel model should not only provide a full description of IoT and massive MIMO channel characteristics, but also other scenarios, such as UAV, V2V, HST, etc. [146], [147], [148], [149], [150]. In addition, massive MIMO using RIS is a new topic to improve system coverage. The standard pervasive channel model can be a combination of RT, GBSM, and AI/ML-based channel models. It should provide fair tradeoff among accuracy, complexity, and pervasiveness/universality. Based on the pervasive channel model, reasonable comparisons of different algorithms and technologies can be obtained.

VI. CONCLUSION

In this article, two mainstream massive MIMO channel model classification methods, i.e., physical versus analytical and deterministic versus stochastic methods, have been thoroughly compared. A more inclusive and clear massive MIMO channel model classification framework has been proposed, i.e., AI/ML-based predictive channel models and classical non-predictive channel models, which utilizes deterministic versus stochastic method but combines physical versus analytical method with clear boundaries. This will allow researchers to choose massive MIMO channel models based on different applications. Existing massive MIMO channel measurement campaigns and advanced channel modeling works have been fully reviewed. It has been concluded that extensive channel measurements and characteristic analyses should be conducted in the future. The necessity of a pervasive massive MIMO channel model that considers all frequency bands and all scenarios has also been emphasized.

REFERENCES

- [1] C.-X. Wang, J. Huang, H. Wang, X. Q. Gao, X.-H. You, and Y. Hao, "6G wireless channel measurements and models: Trends and challenges," *IEEE Veh. Technol. Mag.*, vol. 15, no. 4, pp. 22–32, Dec. 2020.
- [2] X.-H. You *et al.*, "Towards 6G wireless communication networks: Vision, enabling technologies, and new paradigm shifts," *Sci. China Inf. Sci.*, vol. 64, no. 1, Jan. 2021, Art. no. 110301, doi: [10.1007/s11432-020-2955-6](https://doi.org/10.1007/s11432-020-2955-6).

- [3] K. Zheng, S. Ou, and X. Yin, "Massive MIMO channel models: A survey," *Int. J. Antennas Propag.*, vol. 2014, pp. 1–10, Jun. 2014.
- [4] Ö. Özdogan, E. Björnson, and E. G. Larsson, "Massive MIMO with spatially correlated Rician fading channels," *IEEE Trans. Commun.*, vol. 67, no. 5, pp. 3234–3250, May 2019.
- [5] Y. Han, S. Jin, C.-K. Wen, and X. Ma, "Channel estimation for extremely large-scale massive MIMO systems," *IEEE Wireless Commun. Lett.*, vol. 9, no. 5, pp. 633–637, May 2020.
- [6] S. Gunnarsson, J. Flordelis, L. Van Der Perre, and F. Tufvesson, "Channel hardening in massive MIMO: Model parameters and experimental assessment," *IEEE Open J. Commun. Soc.*, vol. 1, pp. 501–512, 2020.
- [7] E. Björnson, L. Sanguinetti, H. Wymeersch, J. Hoydis, and T. L. Marzetta, "Massive MIMO is a reality—What is next? Five promising research directions for antenna arrays," Jun. 2019. [Online]. Available: <https://arxiv.org/abs/1902.07678>
- [8] F. Rusek *et al.*, "Scaling up MIMO: Opportunities and challenges with very large arrays," *IEEE Signal Process. Mag.*, vol. 30, no. 1, pp. 40–60, Jan. 2013.
- [9] E. G. Larsson, O. Edfors, F. Tufvesson, and T. L. Marzetta, "Massive MIMO for next generation wireless systems," *IEEE Commun. Mag.*, vol. 52, no. 2, pp. 186–195, Feb. 2014.
- [10] M. Pätzold, *Mobile Radio Channels*. Chichester, U.K.: Wiley, 2012.
- [11] J. Huang, C.-X. Wang, Y. Yang, Y. Liu, J. Sun, and W. Zhang, "Channel measurements and modeling for 400–600 MHz bands in urban and suburban scenarios," *IEEE Internet Things J.*, vol. 8, no. 7, pp. 5531–5543, Apr. 2021.
- [12] R. O. Schmidt, "Multiple emitter location and signal parameter estimation," *IEEE Trans. Antennas Propag.*, vol. AP-34, no. 3, pp. 276–280, Mar. 1986.
- [13] B. H. Fleury, M. Tschudin, R. Heddergott, D. Dahlhaus, and K. I. Pedersen, "Channel parameter estimation in mobile radio environments using the SAGE algorithm," *IEEE J. Sel. Areas Commun.*, vol. 17, no. 3, pp. 434–450, Mar. 1999.
- [14] R. Feng, J. Huang, J. Sun, and C.-X. Wang, "A novel 3D frequency domain SAGE algorithm with applications to parameter estimation in mmWave massive MIMO indoor channels," *Sci. China Inf. Sci.*, vol. 60, no. 8, pp. 1–12, pp. 58–69, 2017, doi: [10.1007/s11432-017-9139-4](https://doi.org/10.1007/s11432-017-9139-4).
- [15] R. Feng, Y. Liu, J. Huang, J. Sun, C.-X. Wang, and G. Goussetis, "Channel parameter estimation algorithms: Recent advances and future challenges," *China Commun.*, vol. 14, no. 5, pp. 211–228, May 2018.
- [16] D. He, B. Ai, K. Guan, L. Wang, Z. Zhong, and T. Kürner, "The design and applications of high-performance ray-tracing simulation platform for 5G and beyond wireless communications: A tutorial," *IEEE Commun. Surveys Tuts.*, vol. 21, no. 1, pp. 10–27, 1st Quart., 2019.
- [17] L. Liu *et al.*, "The COST 2100 MIMO channel model," *IEEE Wireless Commun. Mag.*, vol. 19, no. 6, pp. 92–99, Dec. 2012.
- [18] "Study on channel model for frequencies from 0.5 to 100 GHz, v14.0.0," 3GPP, Sophia Antipolis, France, Rep. TR 38.901, Mar. 2017.
- [19] P. Kyösti *et al.*, "WINNER II channel models," IST, Rep. IST-4-027756 WINNER II D1.1.2 V1.2, Sep. 2007.
- [20] J. Meinilä, "WINNER + final channel models," WINNER, document Deliverable WINNER + CELTIC/CP5-026 D5.3 V1.0, Jun. 2010.
- [21] A. Maltsev *et al.*, "Channel modeling and characterization," MiWEBA, Breitengüßbach, Germany, document Deliverable MiWEBA FP7-ICT 368721 D5.1 V1.0, Jun. 2014.
- [22] S. Jaeckel, L. Raschkowski, K. Börner, and L. Thiele, "QuaDRiGa: A 3-D multi-cell channel model with time evolution for enabling virtual field trials," *IEEE Trans. Antennas Propag.*, vol. 62, no. 6, pp. 3242–3256, Jun. 2014.
- [23] C.-X. Wang, J. Bian, J. Sun, W. Zhang, and M. Zhang, "A survey of 5G channel measurements and models," *IEEE Commun. Surveys Tuts.*, vol. 20, no. 4, pp. 3142–3168, 4th Quart., 2018.
- [24] K. Yu and B. Onersten, "Models for MIMO propagation channels: A review," *Wireless Commun. Mobile Comput.*, vol. 50, no. 5, pp. 653–666, Oct. 2002.
- [25] P. Almers *et al.*, "Survey of channel and radio propagation models for wireless MIMO systems," *EURASIP J. Wireless Commun. Netw.*, vol. 2007, no. 1, pp. 1–19, Feb. 2007.
- [26] J. Brady, N. Behdad, and A. M. Sayeed, "Beamspace MIMO for millimeter-wave communications: System architecture, modeling, analysis, and measurements," *IEEE Trans. Antennas Propag.*, vol. 61, no. 7, pp. 3814–3827, Jul. 2013.
- [27] C. Sun, X. Q. Gao, S. Jin, Z. Ding, and C. Xiao, "Beam division multiple access transmission for massive MIMO communications," *IEEE Trans. Commun.*, vol. 63, no. 6, pp. 2170–2184, Jun. 2015.
- [28] L. You, X.-Q. Gao, G. Li, X.-G. Xia, and N. Ma, "BDMA for millimeter-wave/Terahertz massive MIMO transmission with per-beam synchronization," *IEEE J. Sel. Areas Commun.*, vol. 35, no. 7, pp. 1550–1563, Jul. 2017.
- [29] A. M. Sayeed, "Deconstructing multi-antenna fading channels," *IEEE Trans. Signal Process.*, vol. 50, no. 10, pp. 2563–2579, Oct. 2002.
- [30] C.-X. Wang, X. Hong, H. Wu, and W. Xu, "Spatial temporal correlation properties of the 3GPP spatial channel model and the Kronecker MIMO channel model," *EURASIP J. Wireless Commun. Netw.*, vol. 2007, pp. 1–9, Jan. 2007.
- [31] X. You and Y. Wang, "Massive MIMO channel modeling," M.S. thesis, Dept. Comput. Sci., Lund Univ., Lund, Sweden, Dec. 2015.
- [32] H. Özcelik, N. Czink, and E. Bonek, "What makes a good MIMO channel model?" in *Proc. IEEE VTC*, Stockholm, Sweden, May 2005, pp. 156–160.
- [33] Y. Zhang *et al.*, "A general coupling-based model framework for wide-band MIMO channels," *IEEE Trans. Antennas Propag.*, vol. 60, no. 2, pp. 574–586, Feb. 2012.
- [34] C. Wen, S. Jin, and K. Wong, "On the sum-rate of multiuser MIMO uplink channels with jointly-correlated Rician fading," *IEEE Trans. Commun.*, vol. 59, no. 10, pp. 2883–2895, Oct. 2011.
- [35] I. Trindade, F. Müller, and A. Klautau, "Accuracy analysis of the geometrical approximation of MIMO channels using ray-tracing," in *Proc. IEEE LATINCOM*, Nov. 2020, pp. 1–5.
- [36] F. Lai, C.-X. Wang, J. Huang, X. Q. Gao, and F. Zheng, "A novel massive MIMO beam domain channel model," in *Proc. IEEE WCNC*, Seoul, South Korea, May 2020, pp. 1–6.
- [37] M. M. Taygur and T. F. Eibert, "Characterization of frequency-selective massive MIMO channels by ray-tracing," in *Proc. EuCAP*, Krakow, Poland, Mar. 2019, pp. 1–5.
- [38] S. Hur *et al.*, "28 GHz channel modeling using 3D ray-tracing in urban environments," in *Proc. EuCAP*, Lisbon, Portugal, May 2015, pp. 1–5.
- [39] M. M. Taygur and T. F. Eibert, "Investigations on massive MIMO performance with multi-antenna users by ray-tracing," in *Proc. IEEE PIMRC*, Istanbul, Turkey, Sep. 2019, pp. 1–6.
- [40] Q. Yao, Y. Yuan, A. Ghazal, C.-X. Wang, L. Luan, and X. Lu, "Comparison of the statistical properties of the LTE-A and IMT-A channel models," in *Proc. IEEE WCNC*, Paris, France, Apr. 2012, pp. 1–6.
- [41] M. Matthaiou, "Characterisation and modelling of indoor and short-range MIMO communications," Ph.D. dissertation, Dept. Comput. Sci., Univ. Edinburgh, Edinburgh, U.K., Nov. 2008.
- [42] A. Imoize, A. Ibhaze, A. Atayero, and K. Kavitha, "Standard propagation channel models for MIMO communication systems," *Wireless Commun. Mobile Comput.*, vol. 2021, pp. 1–36, Feb. 2021.
- [43] C.-X. Wang, Z. Lv, X. Q. Gao, X.-H. You, Y. Hao, and H. Haas, "Pervasive channel modeling theory and applications to 6G GBSMs for all frequency bands and all scenarios," *IEEE Trans. Veh. Technol.*, early access, Jun. 2, 2022, doi: [10.1109/TVT.2022.3179695](https://doi.org/10.1109/TVT.2022.3179695).
- [44] J. Huang, Y. Liu, C.-X. Wang, J. Sun, and H. Xiao, "5G millimeter-wave channel sounders, measurements, and models: Recent developments and future challenges," *IEEE Commun. Mag.*, vol. 57, no. 1, pp. 138–145, Jan. 2019.
- [45] T. Rappaport, Y. Xing, G. R. MacCartney, A. F. Molisch, E. Mellios, and J. Zhang, "Overview of millimeter wave communications for fifth-generation (5G) wireless networks—with a focus on propagation models," *IEEE Trans. Antennas Propag.*, vol. 65, no. 12, pp. 6213–6230, Dec. 2017.
- [46] C. Han and Y. Chen, "Propagation modeling for wireless communications in the Terahertz band," *IEEE Commun. Mag.*, vol. 56, no. 6, pp. 96–101, Jun. 2018.
- [47] Y. Liu, C.-X. Wang, and J. Huang, "Recent developments and future challenges in channel measurements and models for 5G and beyond high-speed train communication systems," *IEEE Commun. Mag.*, vol. 57, no. 9, pp. 50–56, Sep. 2019.
- [48] Y. Liu, A. Ghazal, C.-X. Wang, X. Ge, Y. Yang, and Y. Zhang, "Channel measurements and models for high-speed train wireless communication systems in tunnel scenarios: A survey," *Sci. China Inf. Sci.*, vol. 60, no. 10, p. 17, Oct. 2017.
- [49] P. Zhang, J. Chen, X. Yang, N. Ma, and Z. Zhang, "Recent research on massive MIMO propagation channels: A survey," *IEEE Commun. Mag.*, vol. 56, no. 12, pp. 22–29, Dec. 2018.
- [50] J. Zhang, C. Wang, Z. Wu, and W. Zhang, "A survey of massive MIMO channel measurements and models," *ZTE Commun.*, vol. 15, no. 1, pp. 14–22, Feb. 2017.

- [51] C.-X. Wang, S. Wu, L. Bai, X. You, J. Wang, and C.-L. I, "Recent advances and future challenges for massive MIMO channel measurements and models," *Sci. China Inf. Sci.*, vol. 59, no. 2, pp. 1–16, Feb. 2016.
- [52] A. Saleh and R. Valenzuela, "A statistical model for indoor multipath propagation," *IEEE J. Sel. Area Commun.*, vol. SAC-5, no. 2, pp. 128–137, Feb. 1987.
- [53] H. Özcelik, M. Herdin, W. Weichselberger, J. Wallace, and E. Bonek, "Deficiencies of 'Kronecker' MIMO radio channel model," *Electron. Lett.*, vol. 39, no. 16, pp. 1209–1210, Aug. 2003.
- [54] A. Anderson and H. Haas, "Using echo state networks to characterise wireless channels," in *Proc. IEEE VTC Spring*, Dresden, Germany, Jun. 2013, pp. 1–5.
- [55] C. Jiang, H. Zhang, Y. Ren, Z. Han, K.-C. Chen, and L. Hanzo, "Machine learning paradigms for next-generation wireless networks," *IEEE Wireless Commun.*, vol. 24, no. 2, pp. 98–105, Apr. 2017.
- [56] Q. Zhu, X. Dang, D. Xu, and X. Chen, "High efficient rejection method for generating Nakagami- m sequences," *Electron. Lett.*, vol. 47, no. 19, pp. 1100–1101, Sep. 2011.
- [57] Q. Zhu *et al.*, "A novel 3D non-stationary wireless MIMO channel simulator and hardware emulator," *IEEE Trans. Commun.*, vol. 66, no. 9, pp. 3865–3878, Sep. 2018.
- [58] L. Liu, C. Tao, D. W. Matolak, Y. Lu, B. Ai, and H. Chen, "Stationarity investigation of a LOS massive MIMO channel in stadium scenarios," in *Proc. IEEE VTC Fall*, Boston, MA, USA, Sep. 2015, pp. 1–5.
- [59] X. Gao, O. Edfors, F. Rusek, and F. Tufvesson, "Massive MIMO performance evaluation based on measured propagation data," *IEEE Trans. Wireless Commun.*, vol. 14, no. 7, pp. 3899–3911, Jul. 2015.
- [60] S. Payami and F. Tufvesson, "Channel measurements and analysis for very large array systems at 2.6 GHz," in *Proc. EUCAP*, Prague, Czech Republic, Mar. 2012, pp. 433–437.
- [61] S. Gunnarsson, J. Flordelis, L. Van der Perre, and F. Tufvesson, "Channel hardening in massive MIMO—A measurement based analysis," in *Proc. IEEE SPAWC*, Kalamata, Greece, Jun. 2018, pp. 1–5.
- [62] D. Fei, R. He, B. Ai, B. Zhang, K. Guan, and Z. Zhong, "Massive MIMO channel measurements and analysis at 3.33 GHz," in *Proc. ChinaCom*, Shanghai, China, Aug. 2015, pp. 194–198.
- [63] C. Wang, J. Zhang, L. Tian, M. Liu, and Y. Wu, "The spatial evolution of clusters in massive MIMO mobile measurement at 3.5 GHz," in *Proc. IEEE VTC Spring*, Sydney, NSW, Australia, Jun. 2017, pp. 1–6.
- [64] L. Hao, J. Rodríguez-Piñeiro, X. Yin, and H. Wang, "Measurement-based massive MIMO polarimetric channel characterization in outdoor environment," *IEEE Access*, vol. 7, pp. 171285–171296, 2019.
- [65] L. Hao *et al.*, "Measurement-based double-directional polarimetric characterization of outdoor massive MIMO propagation channels at 3.5 GHz," in *Proc. IEEE SPAWC*, May 2020, pp. 1–5.
- [66] A. Bernland, M. Gustafsson, C. Gustafson, and F. Tufvesson, "Estimation of spherical wave coefficients from 3-D positioner channel measurements," *IEEE Antennas Wireless Propag. Lett.*, vol. 11, pp. 608–611, 2012.
- [67] Q. Wang *et al.*, "Spatial variation analysis for measured indoor massive MIMO channels," *IEEE Access*, vol. 5, pp. 20828–20840, 2017.
- [68] J. Li, B. Ai, R. He, M. Yang, Z. Zhong, and Y. Hao, "A cluster-based channel model for massive MIMO communications in indoor hotspot scenarios," *IEEE Trans. Wireless Commun.*, vol. 18, no. 8, pp. 3856–3870, Aug. 2019.
- [69] J. Li *et al.*, "The 3D spatial non-stationarity and spherical wavefront in massive MIMO channel measurement," in *Proc. WCSP*, Hangzhou, China, Oct. 2018, pp. 1–6.
- [70] J. Li *et al.*, "Characterization of indoor massive MIMO channel at 11 GHz," in *Proc. URSI GASS*, Montreal, QC, Canada, Aug. 2017, pp. 1–4.
- [71] J. Li *et al.*, "Directional analysis of massive MIMO channels at 11 GHz in theater environment," in *Proc. IEEE VTC Fall*, Aug. 2018, pp. 1–5.
- [72] J. Chen, X. Yin, X. Cai, and S. Wang, "Measurement-based massive MIMO channel modeling for outdoor LoS and NLoS environments," *IEEE Access*, vol. 5, pp. 2126–2140, 2017.
- [73] L. Yao, Y. Liu, and S. Li, "Study on propagation characteristics of outdoor massive MIMO channel based on the SBR method," in *Proc. ICMMT*, Guangzhou, China, May 2019, pp. 1–3.
- [74] A. Mudonhi, R. D' Errico, and C. Oestges, "Indoor mmWave channel characterization with large virtual antenna arrays," in *Proc. EuCAP*, Copenhagen, Denmark, Mar. 2020, pp. 1–5.
- [75] J. Huang, C.-X. Wang, R. Feng, J. Sun, W. Zhang, and Y. Yang, "Multi-frequency mmWave massive MIMO channel measurements and characterization for 5G wireless communication systems," *IEEE J. Sel. Areas Commun.*, vol. 35, no. 7, pp. 1591–1605, Jul. 2017.
- [76] F. Challita, M. Martinez-Ingles, M. Liénard, J. Molina-García-Pardo, and D. P. Gaillot, "Line-of-sight massive MIMO channel characteristics in an indoor scenario at 94 GHz," *IEEE Access*, vol. 6, pp. 62361–62370, 2018.
- [77] S. Li, P. J. Smith, P. A. Dmochowski, H. Tataria, M. Matthaiou, and J. W. Yin, "Massive MIMO for ray-based channels," in *Proc. IEEE ICC*, Shanghai, China, May 2019, pp. 1–7.
- [78] J. X. Li and Y. P. Zhao, "Channel characterization and modeling for large-scale antenna systems," in *Proc. ISCIT*, Incheon, South Korea, Sep. 2014, pp. 559–563.
- [79] Z. Yuan, J. Zhang, Y. Zhang, P. Tang, and L. Tian, "A novel complex PCA-based wireless MIMO channel modeling methodology," in *Proc. VTC Fall*, Dec. 2020, pp. 1–5.
- [80] J. Huang *et al.*, "A big data enabled channel model for 5G wireless communication systems," *IEEE Trans. Big Data*, vol. 6, no. 2, pp. 211–222, Jun. 2020.
- [81] C. Huang *et al.*, "Artificial intelligence enabled radio propagation for communications—Part II: Scenario identification and channel modeling," *IEEE Trans. Antennas Propag.*, vol. 70, no. 6, pp. 3955–3969, Jun. 2022.
- [82] S. Sangodoyin *et al.*, "Cluster characterization of 3-D MIMO propagation channel in an urban macrocellular environment," *IEEE Trans. Wireless Commun.*, vol. 17, no. 8, pp. 5076–5091, Aug. 2018.
- [83] B. Ai *et al.*, "On indoor millimeter wave massive MIMO channels: Measurement and simulation," *IEEE J. Sel. Areas Commun.*, vol. 35, no. 7, pp. 1678–1690, Jul. 2017.
- [84] P. Kyösti, J. Lehtomäki, J. Medbo, and M. Latva-Aho, "Map-based channel model for evaluation of 5G wireless communication systems," *IEEE Trans. Antennas Propag.*, vol. 65, no. 12, pp. 6491–6504, Dec. 2017.
- [85] M. M. Tamaddondar and N. Noori, "Cluster based massive MIMO channel model for indoor environment using ray tracing technique," in *Proc. IEEE APMC*, Kuala Lumpur, Malaysia, Nov. 2017, pp. 1030–1033.
- [86] M. M. Tamaddondar and N. Noori, "3D massive MIMO channel modeling with cluster based ray tracing method," in *Proc. ICEE*, Yazd, Iran, Apr. 2019, pp. 1249–1253.
- [87] S. Wu, C.-X. Wang, H. Aggoune, and M. M. Alwakeel, "A novel Kronecker-based stochastic model for massive MIMO channels," in *Proc. IEEE ICC*, Shenzhen, China, Nov. 2015, pp. 1–6.
- [88] M. Zhai, J. Li, Y. Liang, T. Li, G. Gui, and F. Li, "A novel coupling mode based 3D MIMO channel modeling and capacity analysis for 5G," in *Proc. ICUWB*, Nanjing, China, Oct. 2016, pp. 1–4.
- [89] M. Matthaiou, H. Q. Ngo, P. J. Smith, H. Tataria, and S. Jin, "Massive MIMO with a generalized channel model: Fundamental aspects," in *Proc. IEEE SPAWC*, Cannes, France, Jul. 2019, pp. 1–5.
- [90] K. Dovelos, M. Matthaiou, H. Q. Ngo, and B. Bellalta, "Massive MIMO with multi-antenna users under jointly correlated Ricean fading," in *Proc. IEEE ICC*, Dublin, Ireland, Jun. 2020, pp. 1–6.
- [91] X. Gao, F. Tufvesson, and O. Edfors, "Massive MIMO channels—Measurements and models," in *Proc. ACSSC*, Nov. 2013, pp. 280–284.
- [92] A. O. Martínez, P. Eggers, and E. De Carvalho, "Geometry-based stochastic channel models for 5G: Extending key features for massive MIMO," in *Proc. IEEE PIMRC*, Valencia, Spain, Sep. 2016, pp. 1–6.
- [93] F. Ademaj, S. Schwarz, T. Berisha, and M. Rupp, "A spatial consistency model for geometry-based stochastic channels," *IEEE Access*, vol. 7, pp. 183414–183427, 2019.
- [94] J. Flordelis, X. Li, O. Edfors, and F. Tufvesson, "Massive MIMO extensions to the COST 2100 channel model: Modeling and validation," *IEEE Trans. Wireless Commun.*, vol. 19, no. 1, pp. 380–394, Jan. 2020.
- [95] Y. Zhang, X. Li, L. H. Pang, Y. He, G. Ren, and J. Li, "A 2-D geometry-based stochastic channel model for 5G massive MIMO communications in real propagation environments," *IEEE Syst. J.*, vol. 15, no. 1, pp. 307–318, Mar. 2021.
- [96] Y. Xie, B. Li, X. Zuo, M. Yang, and Z. Yan, "A 3D geometry-based stochastic model for 5G massive MIMO channels," in *Proc. QSHINE*, Taiwan, China, Aug. 2015, pp. 216–222.
- [97] Y. Chen, Y. Li, S. Sun, X. Cheng, and X. Chen, "A twin-multi-ring channel model for massive MIMO system," in *Proc. ISCIT*, Qingdao, China, Sep. 2016, pp. 606–610.
- [98] J. Chen, P. Zhang, X. Zhang, X. Yang, and N. Ma, "A novel 3D multi-confocal ellipsoid simulation model for 5G massive MIMO mobile wireless networks," in *Proc. IEEE GlobeCom*, Abu Dhabi, UAE, Dec. 2018, pp. 1–7.
- [99] M. Wang, N. Ma, J. Chen, and B. Liu, "A novel geometry-based MIMO channel model for vehicle-to-vehicle communication systems," in *Proc. IEEE ICC*, Chengdu, China, Dec. 2019, pp. 762–767.

- [100] C. F. López and C.-X. Wang, "A study of 2D non-stationary massive MIMO channels by transformation of delay and angular power spectral densities," *IEEE Trans. Veh. Technol.*, vol. 69, no. 12, pp. 14212–14224, Dec. 2020.
- [101] C. Liao and K. Xu, "3D stochastic geometry channel model of cell-free massive MIMO system," in *Proc. WCSP*, Nanjing, China, Oct. 2020, pp. 504–509.
- [102] A. Al-Kinani *et al.*, "A 3D non-stationary GBSM for vehicular visible light communication channels," *IEEE Access*, vol. 8, pp. 140333–140347, 2020.
- [103] L. Gu, N. Ma, J. Chen, L. Wang, and B. Liu, "A novel 3D wideband geometry-based channel model for 5G massive MIMO vehicle-to-vehicle communications in urban merging areas," in *Proc. IEEE ICC Wkshps*, Dublin, Ireland, Jun. 2020, pp. 1–6.
- [104] S. Wu, C.-X. Wang, H. Haas, H. Aggoune, M. M. Alwakeel, and B. Ai, "A non-stationary wideband channel model for massive MIMO communication systems," *IEEE Trans. Wireless Commun.*, vol. 14, no. 3, pp. 1434–1446, Mar. 2015.
- [105] C. F. López and C.-X. Wang, "Novel 3D non-stationary wideband models for massive MIMO channels," *IEEE Trans. Wireless Commun.*, vol. 17, no. 5, pp. 2893–2905, May 2018.
- [106] J. Bian, C.-X. Wang, X. Q. Gao, X.-H. You, and M. Zhang, "A general 3D non-stationary wireless channel model for 5G and beyond," *IEEE Trans. Wireless Commun.*, vol. 39, no. 4, pp. 3211–3224, May 2021.
- [107] Y. Sun, C.-X. Wang, J. Huang, and J. Wang, "A 3D non-stationary channel model for 6G wireless systems employing intelligent reflecting surfaces with practical phase shifts," *IEEE Trans. Cogn. Commun. Netw.*, vol. 7, no. 2, pp. 496–510, Jun. 2021.
- [108] J. Wang, C.-X. Wang, J. Huang, H. Wang, and X. Gao, "A general 3D space-time-frequency non-stationary THz channel model for 6G ultra massive MIMO wireless communication systems," *IEEE J. Sel. Areas Commun.*, vol. 39, no. 6, pp. 1576–1589, Jun. 2021.
- [109] X. Cheng, Y. Li, C.-X. Wang, X. Yin, and D. W. Matolak, "A 3D geometry based stochastic model for unmanned aerial vehicle MIMO Ricean fading channels," *IEEE Internet Things J.*, vol. 7, no. 9, pp. 8674–8687, Sep. 2020.
- [110] Y. Liu, C.-X. Wang, H. Chang, Y. He, and J. Bian, "A novel non-stationary 6G UAV channel model for maritime communications," *IEEE J. Sel. Areas Commun.*, vol. 39, no. 10, pp. 2992–3005, Oct. 2021.
- [111] H. Chang *et al.*, "A novel non-stationary 6G UAV-to-ground wireless channel model with 3D arbitrary trajectory changes," *IEEE Internet Things J.*, vol. 8, no. 12, pp. 9865–9877, Jun. 2021.
- [112] X. Wu, X. Yang, S. Ma, B. Zhou, and G. Yang, "Hybrid channel estimation for UPA-assisted millimeter-wave massive MIMO IoT systems," *IEEE Internet Things J.*, vol. 9, no. 4, pp. 2829–2842, Feb. 2022.
- [113] G. Li, C. Sun, E. A. Jorswieck, J. Zhang, A. Hu, and Y. Chen, "Sum secret key rate maximization for TDD multi-user massive MIMO wireless networks," *IEEE Trans. Inf. Forensics Security*, vol. 16, no. 1, pp. 968–982, Sep. 2021.
- [114] V. Bhatia, M. R. Tripathy, and P. Ranjan, "Deep learning for massive MIMO: Challenges and future prospects," in *Proc. IEEE CSNT*, Gwalior, India, Apr. 2020, pp. 26–31.
- [115] X. Zhao *et al.*, "Neural network and GBSM based time-varying and stochastic channel modeling for 5G millimeter wave communications," *China Commun.*, vol. 16, no. 6, pp. 80–90, Jun. 2019.
- [116] Y. Chen and C. Han, "Deep CNN-based spherical-wave channel estimation for terahertz ultra-massive MIMO systems," in *Proc. IEEE GlobeCom*, Taiwan, China, Dec. 2020, pp. 1–6.
- [117] J. W. McKown and R. L. Hamilton, "Ray tracing as a design tool for radio networks," *IEEE Netw.*, vol. 5, no. 6, pp. 27–30, Nov. 1991.
- [118] H.-W. Son and N.-H. Myung, "A deterministic ray tube method for microcellular wave propagation prediction model," *IEEE Trans. Antennas Propagat.*, vol. 47, no. 8, pp. 1344–1350, Aug. 1999.
- [119] J. P. Rossi, J. C. Bic, A. J. Levy, Y. Gabillett, and M. Rosen, "A ray launching method for radio-mobile propagation in urban area," in *Proc. APS*, Jun. 1991, pp. 1540–1543.
- [120] F. A. Agelet, A. Formella, J. M. H. Rabanos, F. I. de Vicente, and F. P. Fontan, "Efficient ray-tracing acceleration techniques for radio propagation modeling," *IEEE Trans. Veh. Technol.*, vol. 49, no. 6, pp. 2089–2104, Nov. 2000.
- [121] V. Degli-Esposti, "Ray tracing propagation modelling: Future prospects," in *Proc. EuCAP*, The Hague, The Netherlands, Apr. 2014, pp. 2232–2232.
- [122] "Study on evaluation methodology of new Vehicle-to-Everything (V2X) use cases for LTE and NR, v15.3.0," 3GPP, Sophia Antipolis, France, Rep. TR 37.885, 2019.
- [123] W. Weichselberger, M. Herdin, H. Özcelik, and E. Bonek, "A stochastic MIMO channel model with joint correlation at both link ends," *IEEE Trans. Wireless Commun.*, vol. 5, no. 1, pp. 90–100, Jan. 2006.
- [124] W. Weichselberger, "On the decomposition of the MIMO channel correlation tensor," in *Proc. IEEE WSA*, Munich, Germany, Mar. 2004, pp. 268–273.
- [125] C. N. Chuah, J. M. Kahn, and D. Tse, "Capacity of multi-antenna array systems in indoor wireless environment," in *Proc. IEEE GLOBECOM*, Sydney, NSW, Australia, Nov. 1998, pp. 1894–1899.
- [126] X. Li, E. Björnson, S. Zhou, and J. Wang, "Massive MIMO with multi-antenna users: When are additional user antennas beneficial?" in *Proc. IEEE ICT*, Thessaloniki, Greece, May 2016, pp. 1–6.
- [127] M. T. A. Rana, R. Vesilo, and A. Saadat, "Antenna selection for massive MIMO Kronecker channel models using non-central principal component analysis," in *Proc. ITNAC*, Nov. 2017, pp. 1–7.
- [128] X. Gao, "Massive MIMO in real propagation environments," Ph.D. dissertation, Dept. Comput. Sci., Lund Univ., Lund, Sweden, Jan. 2016.
- [129] W. Weichselberger, H. Özcelik, M. Herdin, and E. Bonek, "A novel stochastic MIMO channel model and its physical interpretation," in *Proc. WPMC*, Yokosuka, Japan, Oct. 2003, pp. 1–6.
- [130] Y. Yu *et al.*, "Measurement and empirical modeling of massive MIMO channel matrix in real indoor environment," in *Proc. WCSP*, Yangzhou, China, Oct. 2016, pp. 1–5.
- [131] S. Wu, C.-X. Wang, H. Aggoune, M. M. Alwakeel, and Y. He, "A non-stationary 3D wideband twin-cluster model for 5G massive MIMO channels," *IEEE J. Sel. Areas Commun.*, vol. 32, no. 6, pp. 1207–1218, Jun. 2014.
- [132] C. F. López, C.-X. Wang, and Y. Zheng, "A 3D non-stationary wideband massive MIMO channel model based on ray-level evolution," *IEEE Trans. Commun.*, vol. 70, no. 1, pp. 621–634, Jan. 2022.
- [133] A. M. Sayeed and J. Brady, "Beamspace MIMO channel modeling and measurement: Methodology and results at 28 GHz," in *Proc. IEEE GC Wkshps*, Washington, DC, USA, Dec. 2016, pp. 1–6.
- [134] A. M. Sayeed, "MIMO wireless channels made simple," in *Proc. IEEE ISCAS*, May 2002, pp. 861–864.
- [135] A. M. Sayeed, "A virtual MIMO channel representation and applications," in *Proc. IEEE MILCOM*, Boston, MA, USA, Oct. 2003, pp. 615–620.
- [136] S. Noh, M. D. Zoltowski, Y. Sung, and D. J. Love, "Pilot beam pattern design for channel estimation in massive MIMO systems," *IEEE J. Sel. Topics Signal Process.*, vol. 8, no. 5, pp. 787–801, Oct. 2014.
- [137] M. D. Zoltowski, M. Haardt, and C. P. Mathews, "Closed-form 2-D angle estimation with rectangular arrays in element space or beamspace via Unitary ESPRIT," *IEEE Trans. Signal Process.*, vol. 44, no. 2, pp. 316–328, Feb. 1996.
- [138] L. Bai *et al.*, "Performance comparison of six massive MIMO channel models," in *Proc. IEEE/CIC ICC*, Qingdao, China, Oct. 2017, pp. 1–5.
- [139] S. Pratschner *et al.*, "A spatially consistent MIMO channel model with adjustable K factor," *IEEE Access*, vol. 7, pp. 110174–110186, 2019.
- [140] B. H. Fleury, "First- and second-order characterization of direction dispersion and space selectivity in the radio channel," *IEEE Trans. Inf. Theory*, vol. 46, no. 6, pp. 2027–2044, Sep. 2000.
- [141] S. Dahiya, "A statistical block fading channel model for multiuser massive MIMO system," in *Proc. SPCOM*, Bengaluru, India, Jun. 2016, pp. 1–5.
- [142] J. Zhang, Y. Zhang, Y. Yu, R. Xu, Q. Zheng, and P. Zhang, "3-D MIMO: How much does it meet our expectations observed from channel measurements?" *IEEE J. Sel. Areas Commun.*, vol. 35, no. 8, pp. 1887–1903, Aug. 2017.
- [143] E. D. Carvalho, A. Ali, A. Amiri, M. Angjelichinoski, and R. W. Heath, "Non-stationarities in extra-large-scale massive MIMO," *IEEE Wireless Commun.*, vol. 27, no. 4, pp. 74–80, Aug. 2020.
- [144] Á. O. Martínez, E. De Carvalho, and J. Ø. Nielsen, "Towards very large aperture massive MIMO: A measurement based study," in *Proc. GC Wkshps*, Dec. 2014, pp. 281–286.
- [145] A. Al-Kinani, C.-X. Wang, L. Zhou, and W. Zhang, "Optical wireless communication channel measurements and models," *IEEE Commun. Surveys Tuts.*, vol. 20, no. 3, pp. 1939–1962, 3rd Quart., 2018.
- [146] J. C.-W. Lin, G. Srivastava, Y. Zhang, Y. Djenouri, and M. Aloqaily, "Privacy-preserving multiobjective sanitization model in 6G IoT environments," *IEEE Internet Things J.*, vol. 8, no. 7, pp. 5340–5349, Apr. 2021.
- [147] S. Chen, H. Xu, D. Liu, B. Hu, and H. Wang, "A vision of IoT: Applications, challenges, and opportunities with China perspective," *IEEE Internet Things J.*, vol. 1, no. 4, pp. 349–359, Aug. 2014.

- [148] C. Huang, A. F. Molisch, Y. Geng, R. He, B. Ai, and Z. Zhong, "Trajectory-joint clustering algorithm for time-varying channel modeling," *IEEE Trans. Veh. Technol.*, vol. 69, no. 1, pp. 1041–1045, Jan. 2020.
- [149] H. Jiang, W. Ying, J. Zhou, and G. F. Shao, "A 3D wideband two-cluster channel model for massive MIMO vehicle-to-vehicle communications in semi-ellipsoid environments," *IEEE Access*, vol. 8, pp. 23594–23600, 2020.
- [150] C.-X. Wang, A. Ghazal, B. Ai, Y. Liu, and P. Fan, "Channel measurements and models for high-speed train communication systems: A survey," *IEEE Commun. Survey Tuts.*, vol. 18, no. 2, pp. 974–987, 2nd Quart., 2016.



Rui Feng (Member, IEEE) received the B.Sc. degree in communication engineering and the M.Eng. degree in signal and information processing from Yantai University, Yantai, China, in 2011 and 2014, respectively, and the Ph.D. degree in communication and information system from Shandong University, Jinan, China, in 2018.

She was a Lecturer with Ludong University, Yantai, from July 2018 to September 2020. She is currently a Postdoctoral Research Associate with Purple Mountain Laboratories, Nanjing, China, and Southeast University, Nanjing. Her research interests include (ultra) massive MIMO channel modeling theory and beam-domain channel modeling.



Cheng-Xiang Wang (Fellow, IEEE) received the B.Sc. and M.Eng. degrees in communication and information systems from Shandong University, Jinan, China, in 1997 and 2000, respectively, and the Ph.D. degree in wireless communications from Aalborg University, Aalborg, Denmark, in 2004.

He was a Research Assistant with Hamburg University of Technology, Hamburg, Germany, from 2000 to 2001, a Visiting Researcher with Siemens AG Mobile Phones, Munich, Germany, in 2004, and a Research Fellow with the University of Agder, Grimstad, Norway, from 2001 to 2005. He has been with Heriot-Watt University, Edinburgh, U.K., since 2005, where he was promoted to a Professor in 2011. In 2018, he joined Southeast University, Nanjing, China, as a Professor. He is also a part-time Professor with Purple Mountain Laboratories, Nanjing. He has authored 4 books, 3 book chapters, and more than 470 papers in refereed journals and conference proceedings, including 26 highly cited papers. He has also delivered 24 invited keynote speeches/talks and 14 tutorials in international conferences. His current research interests include wireless channel measurements and modeling, 6G wireless communication networks, and electromagnetic information theory.

Dr. Wang received 15 Best Paper Awards from IEEE GLOBECOM 2010, IEEE ICCT 2011, ITST 2012, IEEE VTC 2013 Spring, IWCMC 2015, IWCMC 2016, IEEE/CIC ICC 2016, WPMC 2016, WOCC 2019, IWCMC 2020, WCSP 2020, CSPA 2021, WCSP 2021, and IEEE/CIC ICC 2022, and also the 2020–2022 "AI 2000 Most Influential Scholar Award Honourable Mention" in recognition of his outstanding and vibrant contributions in the field of Internet of Things. He was a Highly Cited Researcher recognized by Clarivate Analytics from 2017 to 2020, and one of the most cited Chinese Researchers recognized by Elsevier in 2021. He is currently an Executive Editorial Committee Member of the IEEE TRANSACTIONS ON WIRELESS COMMUNICATIONS. He has served as an Editor for over ten international journals, including the IEEE TRANSACTIONS ON WIRELESS COMMUNICATIONS from 2007 to 2009, IEEE TRANSACTIONS ON VEHICULAR TECHNOLOGY from 2011 to 2017, and IEEE TRANSACTIONS ON COMMUNICATIONS from 2015 to 2017. He was a Guest Editor of the IEEE JOURNAL ON SELECTED AREAS IN COMMUNICATIONS, Special Issue on *Vehicular Communications and Networks* (Lead Guest Editor), Special Issue on *Spectrum and Energy Efficient Design of Wireless Communication Networks*, and Special Issue on *Airborne Communication Networks*. He was also a Guest Editor of the IEEE TRANSACTIONS ON BIG DATA, Special Issue on *Wireless Big Data*, and is a Guest Editor for the IEEE TRANSACTIONS ON COGNITIVE COMMUNICATIONS AND NETWORKING, Special Issue on *Intelligent Resource Management for 5G and Beyond*. He has served as a TPC member, a TPC chair, and a general chair for more than 80 international conferences. He is a Member of the Academia Europaea (The Academy of Europe) and European Academy of Sciences and Arts, a Fellow of the Royal Society of Edinburgh, IET, and China Institute of Communications, and an IEEE Communications Society Distinguished Lecturer in 2019 and 2020.



Jie Huang (Member, IEEE) received the B.E. degree in information engineering from Xidian University, Xi'an, China, in 2013, and the Ph.D. degree in communication and information systems from Shandong University, Jinan, China, in 2018.

He was a Research Associate with the National Mobile Communications Research Laboratory, Southeast University, Nanjing, China, from October 2018 to October 2020. From January 2019 to February 2020, he was a Research Associate with Durham University, Durham, U.K. He is currently an Associate Professor with the National Mobile Communications Research Laboratory, Southeast University, and also a Researcher with the Purple Mountain Laboratories, Nanjing. His research interests include millimeter wave, THz, massive MIMO, and intelligent reflecting surface channel measurements and modeling, wireless big data, and 6G wireless communications.



Xiqi Gao (Fellow, IEEE) received the Ph.D. degree in electrical engineering from Southeast University, Nanjing, China, in 1997.

He joined the Department of Radio Engineering, Southeast University, in April 1992. He has been a Professor of Information Systems and Communications since May 2001. From September 1999 to August 2000, he was a Visiting Scholar with Massachusetts Institute of Technology, Cambridge, MA, USA, and Boston University, Boston, MA, USA. He visited Darmstadt University of Technology, Darmstadt, Germany, from August 2007 to July 2008, as a Humboldt scholar. His current research interests include broadband multicarrier communications, massive MIMO wireless communications, satellite communications, optical wireless communications, information theory, and signal processing for wireless communications.

Dr. Gao received the Science and Technology Awards of the State Education Ministry of China in 1998, 2006, and 2009, the National Technological Invention Award of China in 2011, the Science and Technology Award of Jiangsu Province of China in 2014, and the 2011 IEEE Communications Society Stephen O. Rice Prize Paper Award in the field of communications theory. From 2007 to 2012, he served as an Editor for the IEEE TRANSACTIONS ON WIRELESS COMMUNICATIONS. From 2009 to 2013, he served as an Associate Editor for the IEEE TRANSACTIONS ON SIGNAL PROCESSING. From 2015 to 2017, he served as an Editor for the IEEE TRANSACTIONS ON COMMUNICATIONS.



Sana Salous (Senior Member, IEEE) received the B.E.E. degree from the American University of Beirut, Beirut, Lebanon, in 1978, and the M.Sc. and Ph.D. degrees from Birmingham University, Birmingham, U.K., in 1979 and 1984, respectively.

She was an Assistant Professor with Yarmouk University, Irbid, Jordan, for four years followed by a one-year Research Fellowship with Liverpool University, Liverpool, U.K. She held a lectureship with the University of Manchester Institute of Science and Technology, Manchester, U.K., in 1989,

where she was subsequently a Senior Lecturer and then a Reader. Since 2003, she has been the Chair of Communications Engineering, Durham University, Durham, U.K., where she is currently the Director of the Centre for Communication Systems. Her current research interests include radio channel characterization in various frequency bands ranging from skywave in the HF band to millimeter-wave bands, design of radar waveforms, and novel radio channel sounders and radar systems for radio imaging.

Dr. Salous was the Chair of the Commission C on Radio Communication and Signal Processing Systems of URSI, from 2014 to 2017. She is the Editor-in-Chief of the *Radio Science*, a publication of the American Geophysical Union. She is a Fellow of the Institution of Engineering and Technology and International Union of Radio Science.



Harald Haas (Fellow, IEEE) received the Ph.D. degree from the University of Edinburgh, Edinburgh, U.K., in 2001.

He is the Director of the LiFi Research and Development Center, University of Strathclyde, Glasgow, U.K. He is also the Initiator, the Co-Founder, and the Chief Scientific Officer of pureLiFi Ltd., Edinburgh. He has authored 550 conference and journal papers, including papers in *Science* and *Nature Communications*. His main research interests are in optical wireless communications, hybrid optical wireless and RF communications, spatial modulation, and interference coordination in wireless networks.

Dr. Haas received the Outstanding Achievement Award from the International Solid State Lighting Alliance in 2016 and the Royal Society Wolfson Research Merit Award. He was a recipient of the IEEE Vehicular Society James Evans Avant Garde Award in 2019. His team invented spatial modulation. He introduced LiFi to the public at an invited TED Global talk in 2011. This talk on Wireless Data from Every Light Bulb has been watched online over 2.72 million times. He was listed among the 50 best inventions in *Time* in 2011. He gave a second TED Global lecture in 2015 on the use of solar cells as LiFi data detectors and energy harvesters. This has been viewed online over 2.75 million times. He was elected a Fellow of the Royal Society of Edinburgh in 2017. In 2018, he received a three-year EPSRC Established Career Fellowship extension and was elected Fellow of IET. He was elected a Fellow of the Royal Academy of Engineering in 2019.